PHYSICAL REVIEW C VOLUME 6, NUMBER 3 SEPTEMBER 1972

Decay of ^{170}Lu to Levels in ^{170}Yb†

David C. Camp*
Lawrence Livermore Laboratory, University of California, Livermore, California 94550

and

Fred M. Bernthal
Departments of Chemistry and Physics, Michigan State University, East Lansing, Michigan 48823
(Received 24 November 1971)

The locations of 70 energy levels in ^{170}Yb were deduced from Compton-suppressed γ-ray singles, three-crystal γ-ray pair, conversion-electron, and Ge(Li)-Ge(Li) γ-γ coincidence measurements on the electron-capture-β^+ decay of ^{170}Lu. Both chemically separated and isotopically separated sources of ^{170}Lu were used in collecting the data. A total of 550 γ-ray transitions have been observed in the ^{170}Lu decay spectrum, 220 of which are definitely assigned to the ^{170}Yb level scheme from 112 coincidence spectra. These definitive transitions account for 93% of the total observed γ-ray intensity. An additional 118 γ-ray transitions were placed on the basis of excited-state energy differences. Eight $E0$ transitions were observed in the conversion-electron data. Each of four excited 0^+ states identified has less than 1% β decay feeding from the 0^+ parent. Spin and parity assignments are proposed for 46 levels in addition to the ground-state rotational band members. The ^{170}Yb level structure is compared with available theoretical calculations, and a preliminary interpretation of several features of the decay scheme is presented.

I. INTRODUCTION

The most complicated radioactive decay yet studied is the electron-capture (EC)-β^+ decay of 2.15-day ^{170}Lu to the levels of ^{170}Yb. Early attempts to interpret the complex γ-ray spectrum from NaI(Tl) data were largely unsuccessful, and until recently, the best available data consisted primarily of conversion-electron spectra.[1-3] With the advent of germanium detectors, however, several groups[4-8] renewed their efforts at unraveling this very complex decay. Hansen and co-workers[9] established 0+ as the ground-state spin and parity of ^{170}Lu. Paperiello *et al.*[10] carried out directional-correlation measurements on several of the more intense transition cascades in this decay and have definitely established the spins of 10 levels in ^{170}Yb. Concurrent with the work reported here were the recent studies reported by Bonch-Osmolovskaya and co-workers[11,12] who employed Ge(Li) detectors, electron-γ, γ-γ, and electron-electron coincidences, in an effort to define the decay scheme. They placed some 177 transitions of 280 seen in the decay, thus accounting for almost 87% of the total γ-ray intensity.

In this work we report the results of extensive γ-ray singles, γ-γ coincidence, and conversion-electron measurements. Compton suppression and three-crystal pair-spectrometer techniques were used to accurately define the energies and intensities of the ^{170}Lu γ-ray transitions. Measurements at lower energies (<1.2 MeV) were carried out with isotopically separated sources. An on-line computer and multiparameter data acquisition system were used in conjunction with two Ge(Li) detectors and an isotopically separated ^{170}Lu source to carry out a detailed study of the γ-γ coincidence spectra. Conversion-electron studies were carried out using chemically separated lutetium sources and a Si(Li) detector. On the basis of these data, we have constructed a level scheme for ^{170}Yb consisting of 70 excited states. Of 550 γ-ray transitions identified, over 200 have been placed on the basis of γ-γ coincidence data and another 118 were placed on the basis of energy differences; these two groups of γ rays account for 93 and 3% of the total γ-ray intensity, respectively. Significant differences exist between our decay scheme and that of Bonch-Osmolovskaya *et al.*,[12] and slight differences distinguish our decay scheme from the less complete level scheme of Mihelich.[13]

II. EXPERIMENTAL

A. Target and Source Preparation

Sources of ^{170}Lu were prepared by the ^{169}Tm$(\alpha, 3n)^{170}$Lu reaction by irradiating 40-mg samples of Tm_2O_3 at the Lawrence Berkeley Laboratory 88-in. cyclotron with 40-MeV α particles. 3-h irradiations at about 20-μA beam current produced about 1 mCi of ^{170}Lu activity for each experiment.

The lutetium activity was separated from other reaction products by ion-exchange chemistry. The target material was dissolved in 3 *M* HCl and placed on a 60-cm-long Dowex 50×8 (150–200 mesh) column; 0.05 *M* α-hydroxy isobutyric acid at *p*H 5.3 was used as the eluting agent. An 8-h elution time allowed essentially complete separation of the lutetium activity from the thulium. The γ-ray sources were prepared by evaporating small amounts of the activity to dryness on aluminum or Teflon[14] backings. Conversion-electron sources were prepared by liquid deposition of the activity onto 0.25-mil gold-anodized Mylar. Source material for the isotope separator was prepared by adding 1 mg of Lu^{+3} carrier, precipitating the hydroxide with 8-hydroxy quinoline, and igniting to form Lu_2O_3. γ-ray sources were obtained from the isotope separator on 5-mil aluminum foil. Counting was usually begun 12 to 24 h after the end of irradiation.

B. Experimental Apparatus

A number of different detector systems were used in this study to obtain the spectral data. These systems include a Compton suppression and three-crystal pair spectrometer, a small Ge(Li) x-ray detector, a γ-γ coincidence system, and a Si(Li) conversion-electron detector system. In addition, ordinary singles Ge(Li) detector data were obtained for the interfering activities by counting isotopically separated sources of ^{169}Lu, ^{171}Lu, and ^{172}Lu.

The Compton suppression and three-crystal pair-

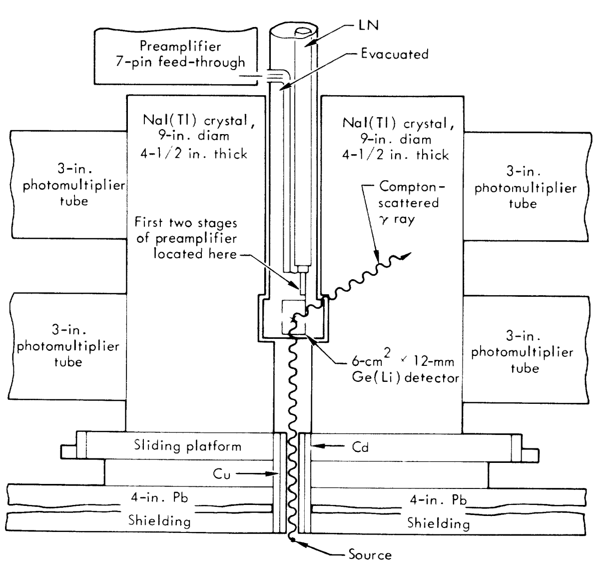

FIG. 1. A schematic drawing of the NaI(Tl) Compton suppression and three-crystal pair spectrometer used in this work.

spectrometer system used in this study is shown schematically in Fig. 1. The central Ge(Li) detector is a planar type, 2.0 by 3.0 cm (6 cm^2), with a 12-mm depletion depth (7 cm^3), oriented such that the 3.0-cm length is colinear with the γ-ray collimation axis. Cooled field-effect transistors in the preamplifier permit resolutions as low as 1.0, 2.0, and 3.0 keV full with at half maximum (FWHM) at 122, 1332, and 2754 keV, respectively. Two 22.9-cm-diam×11.4-cm-thick NaI(Tl) detectors machined to allow maximum enclosure surround the Ge(Li) detector housing. The entire system rests in a cylindrical lead shield with 10.2-cm-thick walls. A 1.9-cm-diam hole reduced to 1.3 cm by cadmium and copper lining collimates incoming γ rays. When the NaI(Tl) detectors are operated in anticoincidence with the Ge(Li) detector, those Compton events that scatter out of the Ge(Li) detector and trigger the NaI(Tl) circuitry are eliminated. For ^{60}Co, the maximum 1.33-MeV full-energy peak-to-minimum continuum ratio observed with this system is 140 : 1 and for ^{137}Cs it is 640 : 1. When the NaI(Tl) detectors are operated independently, and single-channel windows are used to select 511-keV annihilation radiation, the system can also be simultaneously operated as a three-crystal pair spectrometer.

The suppression and three-crystal pair techniques offered by this spectrometer assembly have a number of significant advantages for the measurement of very complex γ-ray spectra such as that of ^{170}Lu. Many weaker radiations, which are ordinarily obscured by the Compton distribution, can be observed. Single- and double-escape peaks, which normally add complexity to the higher-energy portions of γ-ray spectra, are suppressed by factors of 6 and 40, respectively. Thus, the precision obtainable for γ-ray intensities is improved at all energies. Finally, a pair spectrum unequivocally selects only those peaks that are due to γ-ray pair events and thus allows observation of weaker peaks than can be seen in the Compton-suppressed data. A more detailed description of all aspects of this system appears in the work of Camp.[15]

Data from the chemically and isotopically separated sources were also taken with the use of a low-energy photon Ge(Li) system 50 mm^2 in area and 5 mm in depletion depth. This system offers the advantage of very high resolution (600 eV FWHM at 100 keV) and is relatively insensitive to high-energy radiations. The energy region from 0 to 200 keV was observed in detail with this detector.

The γ-γ coincidence system[16] consisted of a 10-cm^3 planar Ge(Li) detector and a 35-cm^3 coaxial Ge(Li) detector coupled with a multiparameter data acquisition system interfaced to a PDP-7 computer. The 4096×4096×512-channel E_{γ_1}-E_{γ_2} time-coincidence distributions were digitized and stored serially on standard IBM magnetic tapes. These data were later sorted and processed, using computer codes developed for the LBL CDC-6600 computer.

Conversion-electron data were obtained with a 3-mm-deep×1-cm^2 Si(Li) detector operated at 650-V bias and at 110°K. The resolution of this system was about 2.7 keV FWHM for the 975.6-keV *K* conversion-electron line of ^{207}Bi.

C. Experimental Data

1. Analysis of the ^{170}Lu γ-Ray Spectra

The γ-ray singles spectra from the ^{170}Lu decay are shown in Figs. 2 and 3. These data include spectra taken both with and without the benefit of isotope-separated sources. Attempts to perform the Lu isotope separation using LuF_3 were at first unsuccessful. In these early experiments, the higher-energy γ-ray data least affected by the interfering ^{169}Lu, ^{171}Lu, and ^{172}Lu activities were obtained from sources not isotopically separated and are shown in Figs. 3 and 4. These data extend from 1200 to 3500 keV and include the Compton-suppressed singles and the "pair" spectra that were accumulated simultaneously with use of the Compton-suppression system. To identify the impurity activities in these early data, successive counts were taken at 2-day intervals.

The low-energy data from the sources that were only chemically separated are not shown here because of the large number of interfering lines from ^{169}Lu and ^{171}Lu decay. Instead, Fig. 2 shows the data acquired from a later source that was isotopically separated. The Lu_2O_3 isotopic separation at that time allowed sufficient activity only for the acquisition of γ-γ coincidence data and the low-energy γ-ray singles data. The successful isotope separation also permitted data to be taken on the

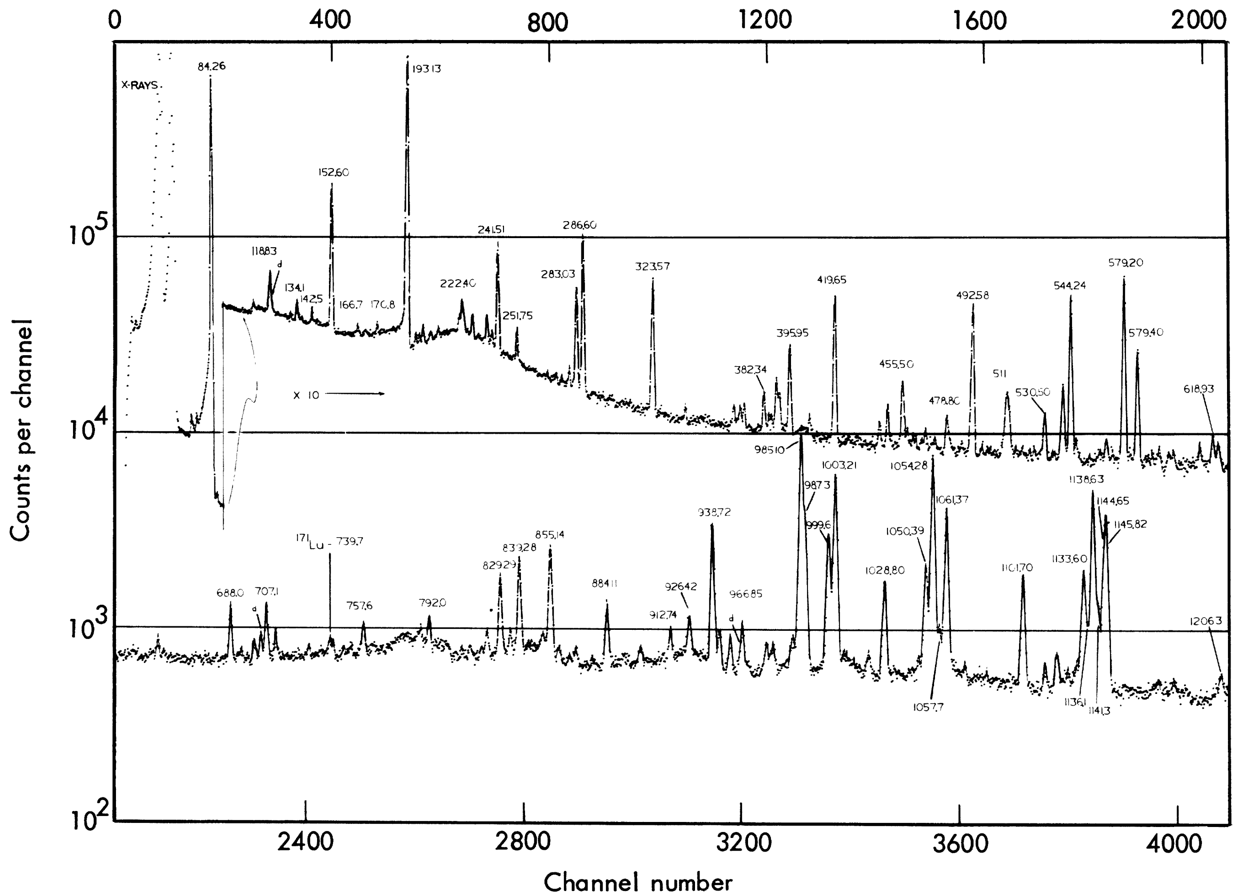

FIG. 2. A low-energy portion of isotopically separated ^{170}Lu γ-ray spectrum taken with the Compton suppression system shown in Fig. 1. A lower-case d shows the presence of a doublet component; an upper-case D indicates the presence of a double-escape peak. Only some of the many transitions observed have been identified.

^{169}Lu, ^{171}Lu, and, later, the ^{172}Lu decays, so positive identification of contaminant peaks and accurate removal of their relative intensities from the earlier mixed-isotope data was possible.

In the low-energy portion (70 keV to 1.2 MeV) of the ^{170}Lu γ-ray spectrum shown in Fig. 2, only some of the peaks have been labeled with their energies. Many others can be identified by comparing the tabulated γ-ray results with this figure. The excellent isotopic separation is shown by the trace amount of ^{171}Lu remaining. The 739.7-keV transition from the ^{171}Lu decay was the most prominent peak above 200 keV in the spectrum from the earlier chemically separated source. Trace amounts of ^{169}Lu and ^{169}Yb activity are also just visible in these data. The strongest indicators of these activities are transitions at 108.9 and 197.8 keV, which in the earlier data were almost half as intense as the 193.1-keV ^{170}Lu transition. Many of the weaker peaks seen in this spectrum and some not seen here at all were visible in the earlier mixed-isotope data which had greater than 10^4 counts in the continuum over this same energy region.

Additional data from the isotopically separated source were obtained in the energy region from 10 to 205 keV with use of the small Ge(Li) x-ray spectrometer. As the ^{170}Lu activity decayed, the trace amounts of ^{169}Lu and ^{171}Lu in this region were easily identified. Also, the higher-energy 119.9-keV component of the 118.8-keV peak was easily observed in these data.

In the higher-energy portion of the spectrum (Fig. 3), the region from 2380 to 3210 keV is scaled down by one decade. Some of the peaks are labeled with their energies, and a few of the more prominent doublet and triplet components are indicated. The few single- and double-escape peaks remaining in this Compton-suppressed spectrum have not been labeled; some are present but are not very prominent. Quantitative data reduction and comparison of these data with those from the "pair" spectrum in Fig. 4 allowed unequivocal identification of real γ-ray transitions. Again

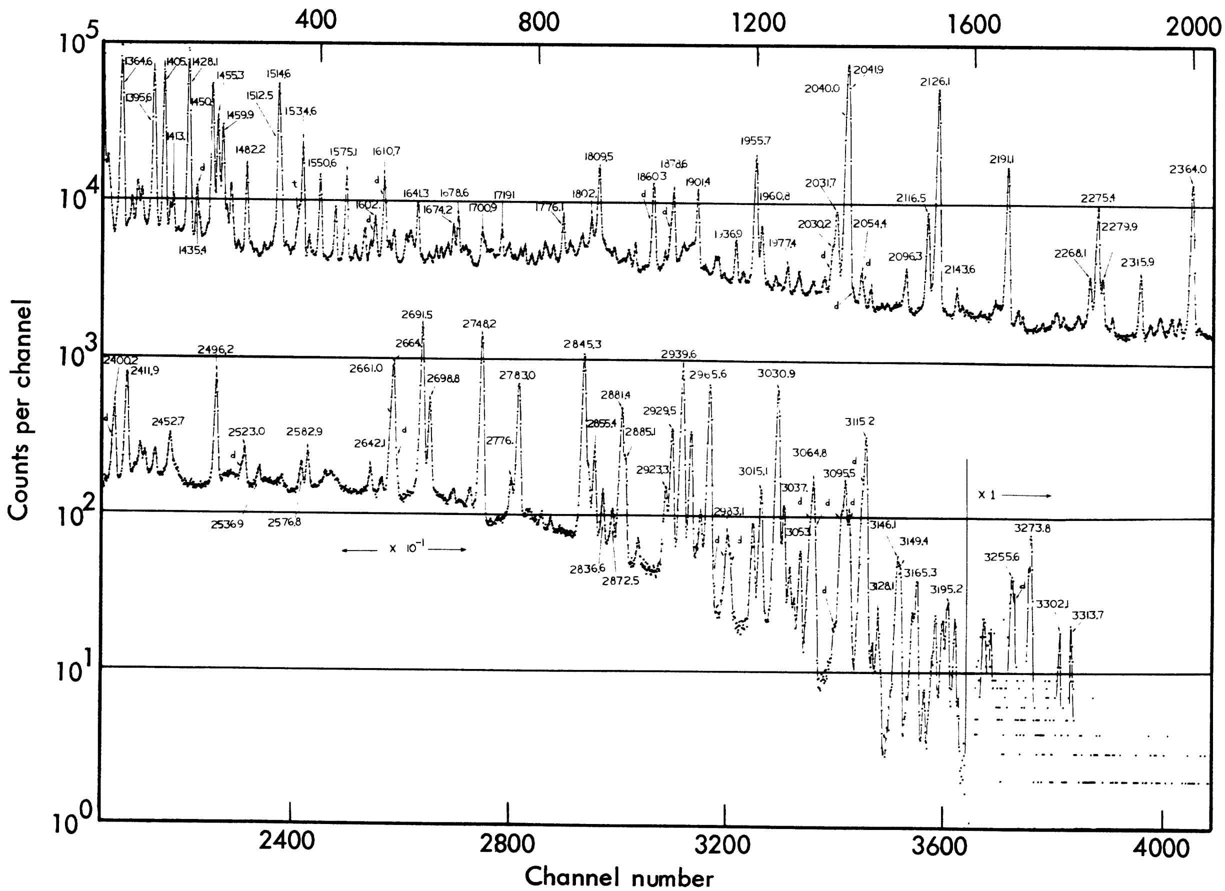

FIG. 3. The high-energy portion of the ^{170}Lu γ-ray spectrum taken with the Compton suppression system. The spectral region from 2380 to 3220 keV has been lowered one decade for clarity of display.

here, only some of the "pair" peaks are labeled with their corresponding transition energies. The energy deposited in the spectrometer by these events is 1022 keV lower than the labels on the peaks, so this spectrum exhibits better resolution than the high-energy Compton suppressed data (e.g., the weak 2046.5-keV component is resolved from the intense 2041.8-keV transition in the "pair" data but not in the suppressed data). The resolution in the high-energy suppressed data varies from 2.2 keV at 1.4 MeV to 4.0 keV at high energies, whereas in the "pair" data it varies from 1.5 to 3.3 keV.

All of the spectral data, including those shown in Figs. 2–4, were analyzed with use of the computer code SAMPO. This code is described in detail elsewhere.[17, 18] The code includes mathematical algorithms for automatically carrying out peak searches, peak fittings, line-shape determinations, and energy and efficiency calibrations. An example of part of the output from this code for the 544-keV multiplet is shown in Fig. 5. Data pertinent to the fit of each peak are tabulated below the graph. The column labeled INTENSITY (CTS) is the area divided by the efficiency. At the end of the spectral printout is a result table summarizing all of the individual fitting data and relative γ-ray intensities. All transition intensities from the ^{170}Lu decay were normalized to the very strong 1364.6-keV transition.

The spectral data shown in Figs. 3 and 4 were analyzed by an on-line interactive method of data reduction. The same code (SAMPO) was used, this time with an interactive graphics system (VISTA)[19] introduced between the user and the CDC-6600 computer.

The intensities from the pair data were first normalized to the Compton-suppressed data using an average normalization factor obtained from the 2040-keV doublet and 2126-keV transitions.

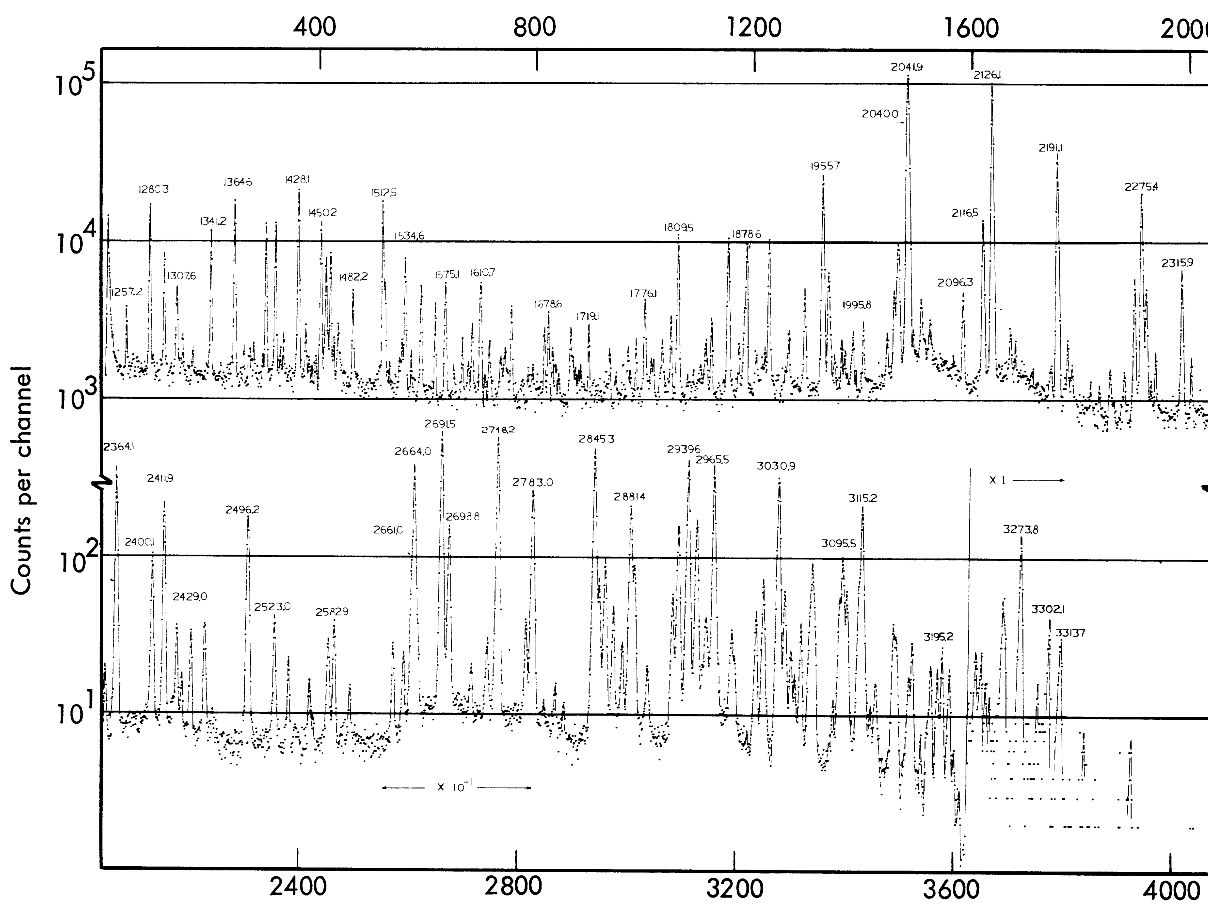

FIG. 4. The "pair" spectrum of ^{170}Lu taken with the system shown in Fig. 1 operated as a three-crystal spectrometer. The spectral region shown as 2350 to 3220 keV has been lowered one decade for clarity of display. Peaks are labeled with their transition energy, not their actual escape-peak energy.

A calibration curve defining the double-escape to full-energy peak ratio for this detector had been established from other data (^{24}Na, ^{56}Co, ^{66}Ga). This curve is a very steep function of energy below 1.5 MeV; hence, the very strong 1280.3-, 1364.6-, and 1428.1-keV transitions were used as secondary normalization points. The intensities for these three transitions were derived from an average of the low- and high-energy (chemically separated) Compton-suppressed data. Pair data for γ rays below 1250 keV were not used in determining final results.

Energy calibrations for all the data obtained in this study were carried out using one of the well-calibrated Ge(Li) detector (singles) systems developed by Gunnink.[20] These systems are used to process many samples on a daily basis and operate continuously with gain stabilization. The nonlinearity function at various conversion gain settings has been precisely measured. The energies of the stronger peaks in the ^{170}Lu data were determined by using these precisely calibrated systems. These energies then served as internal standards in the Compton-suppressed, "pair," and γ-γ coincidence data.

2. ^{170}Lu γ-γ Coincidence Data

Extensive multiparameter γ-γ coincidence information was obtained at 90 and 180° with use of the ^{170}Lu isotopically separated source. The 90° data covered the entire energy region; at 180°, data from the 35-cm^3 detector were accepted only above 800 keV. Some 70 separate coincidence spectra were sorted from the 90° data, and 40 from the 180° data. (Many, but not all, γ-ray gates in the 180° data were the same as in the 90° data.) Both the Compton background coincidences and random coincidences were subtracted by the computer during the sorting process, so the sorted coincidence spectra should represent only "valid" full energy-peak coincidences. The FWHM resolving time of the coincidence time-amplitude curve was 20 nsec; for sorting prompt and random events, digital time gates of about 55 nsec (FWHM) were used.

The large quantity of these data does not allow the display of all of the coincidence spectra here;

CHAN	CONT	DATA	FIT	DEV
1727	785	792	785	.2
1728	781	766	781	-.5
1729	777	774	777	-.1
1730	773	770	773	-.1
1731	769	803	769	1.2
1732	765	777	765	.4
1733	761	781	762	.7
1734	758	730	759	-1.1
1735	754	726	757	-1.2
1736	751	741	758	-.6
1737	748	775	762	.5
1738	745	750	774	-.9
1739	742	820	802	.6
1740	739	851	853	-.1
1741	737	933	927	.2
1742	734	1020	1030	-.3
1743	732	1198	1193	.1
1744	730	1407	1413	-.2
1745	728	1626	1626	.0
1746	726	1765	1732	.8
1747	724	1626	1662	-.9
1748	722	1463	1443	.5
1749	721	1142	1175	-1.0
1750	719	940	957	-.5
1751	718	918	830	2.9
1752	717	831	788	1.5
1753	716	806	795	.4
1754	715	835	853	-.6
1755	714	1002	992	.3
1756	713	1290	1289	.0
1757	713	1900	1912	-.3
1758	712	2942	2908	.6
1759	712	3908	3983	-1.2
1760	712	4617	4680	-.9
1761	712	4697	4629	1.0
1762	712	4026	3861	2.6
1763	712	2710	2773	-1.2
1764	713	1801	1813	-.3
1765	713	1155	1201	-1.4
1766	714	880	931	-1.7
1767	715	785	834	-1.8
1768	716	838	824	.5
1769	717	866	855	.4
1770	718	925	893	1.0
1771	719	881	910	-1.0
1772	720	913	892	.7
1773	722	829	848	-.7
1774	724	797	799	-.1
1775	725	751	762	-.4
1776	727	767	743	.9
1777	729	792	736	2.0
1778	732	736	734	.1
1779	734	733	735	-.1
1780	736	718	737	-.7
CHAN	CONT	DATA	FIT	(D-F)/SQRT.D=DEV

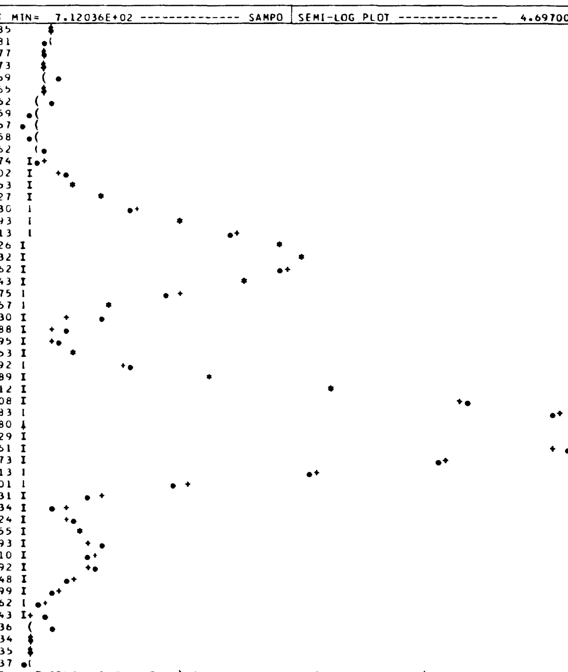

30151=SUM DATA-CONT
30101=SUM FIT-CONT

REJECT FIT AND/OR ERROR ESTIMATES IF CHI SQUARE (4.987E+01) OR SIGMA (1.077) IS LARGE, PERHAPS DUE TO MISSED PEAKS.

CHANNEL--FIT.ERR(CH)		ENERGY-----CAL.ERR-EN.ERR(keV)			AREA-(CTS)----FIT.ERR		INTENSITY-(CTS)--CAL.ERR -INT.ERR		
1742.3897	.5283	539.0360	.0289	.1542	788.422	22.2314	119.334	2.0000	22.3212
1746.2578	.0821	540.1451	.0289	.0373	5476.949	3.3013	831.675	2.0000	3.8599
1760.4378	.0105	544.2108	.0291	.0292	22776.327	.6816	3499.803	2.0000	2.1129
1771.0129	.1522	547.2430	.0292	.0525	1061.260	7.0825	164.511	2.0000	7.3594

FIG. 5. An example of the output from the computer code SAMPO used to analyze the ^{170}Lu low-energy data. The 544-keV region is shown.

TABLE I. γ rays observed in selected coincidence gates at 90 and 180°.

Gated E_γ (keV)	Angle 90°	Angle 180°	γ rays observed in coincidence gate [a]
84.26	X	X	152, 193, 241, 283, 286, 323, 419, 492, 544, 572, 579, 829, 839, 855, 868, 884, 938, 985, 999, 1003, 1028, 1054, 1061, 1101, 1133, 1141, 1144, 1218, 1222, 1225, 1257, 1280, 1294, 1307, 1312, 1341, 1395, 1405, 1428, 1450, 1455, 1459, 1482, 1514, 1550, 1565, 1574, 1610, 1641, 1678, 1719, 1757, 1776, 1809, 1860, 1878, 1901, 1955, 2031, 2041, 2116, 2191, 2205, 2279, 2316, 2411, 2452, 2582, 2664, 2691, 2698, 2845, 2855, 2881, 2885, 2923, 2983, 3015, 3031, (3062), 3065, 3095, 3111
118.8		X	850, 926, 938, 943, 1028, 1222, 1306
152.1	X	X	84, 193, 485, 1028, 1054, 1133, 1144, 1187, 1222, 1242, 1280, 1306, 1341, 1361, 1395, 1438, 1521, 1529, 1597, 2582, 2667
193.13	X	X	84, 118, 152, 228, 283, 419, 455, 479, 492, 544, 572, 572, 706, 741, 819, 829, 868, 947, 966, 980, 1028, 1050, 1057, 1101, 1119, 1218, 1230, 1257, 1350, 1361, 1380, 1395, 1405, 1413, 1469, 1565, 1614, 1630, 1641, 1662, 1759, 1793, 1802, 1842, 1859, 1954
221–4	X		84, 865, 999, 1395, 2191
228.0	X		193, 829, 1028, 1306, 1405
235.6	X		981, 1102, 1222, 1280, 1352, 1428, 1512
241.5	X	X	84, 2041, 2126
251.8	X		193, 2031
283.0	X	X	84, 193, 985, 1002, 1028, 1054, 1138, 1144, 1172, 1222, 1230, 1306+8, 1391, 1398, 1467, 2452, 2536
286.6	X	X	84, 850, 926, 938, 1054, 1138, 1323, 1514, 1531, 1540, 1706
323.6	X	X	84, 983, 1054, 1070, 1138, 1144, 1426+8, 2411, 2496
395.9	X	X	84, 829, 1054, 1138, 1405, 1413
419.6	X	X	84, 193, 1380, 2315, 2400
455.5		X	1057, 1138, 1218, 1225, 1280, 1341, 1428, 1512
447.6	X		84, 576, 741, 1003, 1061, 1222, 1428
479.0	X		84, 96?, 193, 385
492.6	X	X	84, 193, 947, 1050, 1101, 1141
530.5	X		193, 329
544.2	X		84, 850, 910, 985, 1054, 1137, 1206, 1280, 1306, 2191, 2275
572.2	X	X	84, 193, 868, 1050, 1061, 1101, 1145
579.4	X	X	84, 1050, 1054, 1101, 1138
612.1	X		222
688.0	X	X	(84), 916, 1280, 1364
706–8	X		193
829.3	X		193, 1257, 1450, 1534
839.3	X		1428, 1512
855.2	X		84, 1428, 1512

TABLE I *(Continued)*

Gated E_γ (keV)	Angle 90°	180°	γ rays observed in coincidence gate [a]
868.1	X		193, 323,
938.7	X		84, 118, 193, 286, 1054, 1341
947.8	X		193, 492
983.7	X	X	84, (323), 1428
985.1	X	X	84, 1206, 1294, 1678, 1860, 1878, 1995, 2030, 2096
987.3	X		84, 1280, 1364
999.6	X		84, 193?, 1280, 1364
1003.2	X	X	1054, 1145, 1280, 1364
1028.8	X	X	84, 152, 193, 1057, 1361, 1641, 1793, 1842, 1859
1050.4	X	X	84, 193, 492, 572, 579, 1054, 1061, 1138, 1141, 1145
1054.3	X	X	84, 286, 396, 455, 579, 938, 980, 1002, 1050, 1101, 1137, 1225, 1405, 1529, 1609, 1809, 1960, 2027
1061.4	X	X	84, 152, 388, 572, 819, 829, 980, 988, 1002, 1050, 1055, 1101, 1132, 1218, 1405, 1602, 1802, 2041, 2126
1101.7	X	X	193, 492, 572, 579, 1054, 1061, 1138, 1141, 1145
1119.4	X		193
1133.6	X		84, 1280, 1364
1138.6	X		286, 579, 1137, 1225, 1398, 1529, 1609, 1809, 1960, 2027
1144.6	X	X	84, 152, 1135, 1438, 1700, 1719, 1936
1145.8	X	X	572, 1050, 1101, 1132, 1218, 1521, 1802
1218.5	X		84, 193, 1061, 1145
1225.6	X		84, 1054, 1138
1257.2	X	X	84, 193, 829, 1395, 1405, 1413, 1507, 1564
1280.3	X	X	84, 688, 910, 987, 999, 1003, 1133, 1383, 1403, 1455, 1565, 1575, 1601, 1610, 1776
1294.7	X		84, 985
1307.5	X		84, 283, 1428, 1512
1341.2	X	X	84, 926, 938, 942, 1070, 1323, 1514, 1531, 1540, 1549
1364.6	X		[84, 152, 193-via 1361], 987, 999, 1003, 1133, 1455, 1575, 1610, 1776
1380.8	X		193, 419
1395.6	X	X	84, 193, 884, 1268, 1449, 1459, 1467, 1619, 1685
1405.1	X		84, 193, 388, 395, 1257, 1450, 1534
1428.1	X	X	84, 540, 839, 855, 983, 1235, 1263, 1307, 1427, 1435, 1457, 1647
1450.2	X		84, 829, 1132, 1395, 1405
1455.3	X		84, 1280, 1364
1459.9	X	X	84, 1395
1512.5	X		839, 855, 983, 1263, 1307

TABLE I *(Continued)*

Gated E_γ (keV)	Angle 90°	180°	γ rays observed in coincidence gate [a]
1514.6	X		84, 286, 1138, 1341
1550.5		X	1113, 1294, 1304, 1313, 1341
1860	X		84, 193, 985, 1028, 1222
2041.9	X		84, 241,
2116.6			84

[a] A qualitative indication of the relative strengths of the γ rays appearing in each coincidence gate is shown: The strongest lines are underlined, e.g. 193; the medium strength lines are written normally, e.g. 193; the weak lines are underlined partially, e.g. 193. A question mark following an entry indicates that line was observed, but its presence is not understood in that particular gate. Single- and double-escape peaks are not entered.

however, those γ rays observed in each coincidence gate are listed in Table I. A complete catalog of these coincidence spectra can be found in Appendix I of Ref. 21. Several selected representative gates are shown here. Figure 6 shows the gated coincidence spectra obtained at 90° for the two ^{170}Yb ground-band transitions observed at 84.26 and 193.13 keV. These two spectra are somewhat more complex than all of the others obtained. Perhaps more typical of the coincidence spectra are those shown in Fig. 7. These spectra were obtained at the 180° setting and show those γ rays in coincidence with the 152.6-, 688.0-, and 1028.8-keV transitions. The Compton-suppressed singles energy and intensity data had been carefully analyzed before the γ-γ coincidence sorting gates were set; hence, many of the close-lying lines were sorted with awareness of their multiplicity. Analysis of the coincidence data revealed the presence of many doublets that were otherwise unresolvable.

There remains one major unresolved problem in the coincidence relationships, that of the 706.5-keV transition in the 193.1-keV gate. According to the analysis of the singles data, there is a doublet with components at 706.5 and 707.1 keV and intensities of approximately 1650 and 3000 units, respectively. The 193-keV gate contains a peak of approximately 2300 ± 250 intensity units at 707 keV (see Fig. 6). No other coincidence gate shows a 707-keV peak. If the 707-keV line feeds the 277.4-keV 4+0 level directly, a level at 984.5 keV is indicated. Such a state would be below the 1069-keV level thought to be the first excited state above the ground band and would have a spin of at least two units. If part of the very intense 985-keV transition is really a ground-state transition from such a 984.5-keV level, then the level might be expected to feed the 84.26-keV 2+0 level. No γ ray with an intensity greater than 300 units was observed either in the singles data or in the 84.26-keV gated spectrum at 900.2 keV. In addition, no strong γ rays could be found decaying from other levels to a level at 984.5 keV. Therefore, such a placement of the 707-keV transition seems implausible at best.

Another possibility is that the 193-keV transition is a very closely spaced doublet. The only other evidence for such a possibility is the appearance of a 193-keV peak in the 999-keV gate. This transition was established from coincidence data to decay from the 2364-keV 1-1 level to the 1364-keV 1-0 level. This latter level does not decay to the 4+0 ground-band member. Therefore the presence of the 193-keV transition in the 999-keV gate remains puzzling. If the 193-keV transition is indeed a doublet, then the 707- and 999-keV transitions may very well be directly related to it. Such a 193-keV twin could not be very intense, since the net intensity balance for the 277.4-keV level is −400 ± 2400 units in 60 000, consistent with the expected negligible β decay to the 4+ state.

3. ^{170}Lu Conversion-Electron Spectrum

In Fig. 8, portions of the conversion-electron data taken with the 3-mm × 1-cm^2 Si(Li) detector are shown. The top two sections show the 4096-channel low-energy spectrum from 100 to 1500 keV, taken with one of the chemically separated sources. These data were taken very soon after chemical separation so that contaminant peaks, denoted C, from ^{169}Lu and ^{171}Lu were minimal. Only some of the *K* and *L* conversion lines are identified. The 193.1-keV *K* conversion peak is slightly asymmetric because of finite source-thickness effects. The bottom spectrum shows the high-energy portion, 1350 to 2800 keV, taken with a

1600-channel analyzer. Some of the prominent K conversion peaks are identified as well as some of the double-escape or "pair" peaks, D, produced by the more intense γ-ray transitions. A few doublets, d, are also noted.

The energy resolution of the electron detector was approximately 2.7 keV for the 976-keV conversion electrons from ^{207}Bi. A relative detection-efficiency curve was obtained from electron measurements on the following standard sources: ^{109}Cd, ^{203}Hg, ^{113}Sn, ^{207}Bi, ^{137}Cs, ^{54}Mn, and ^{65}Zn. The relative strengths of these sources were determined by γ-ray measurements taken with a Ge(Li) detector of known absolute efficiency.

The two spectra in Fig. 8 were analyzed by hand, using a spectrum stripping technique in which strong singlet conversion lines (e.g. 323-, 938-, 1280-, 1479.9-, and 2126-keV, etc.) were used to define the line shapes. Since the very complex nature of the γ spectrum was known, the use of the conversion data was limited to only those peaks that were well defined and whose intensity errors were less than ±10%.

Conversion coefficients were determined by using the theoretical conversion coefficients of (1) the pure $E2$ ground-rotational band transition at 193.1 keV; (2) the 1138.8-, 1144.6-, 1145.9-, 1395.6-, and 1534.5-keV $E2$ transitions; (3) the 1280- and

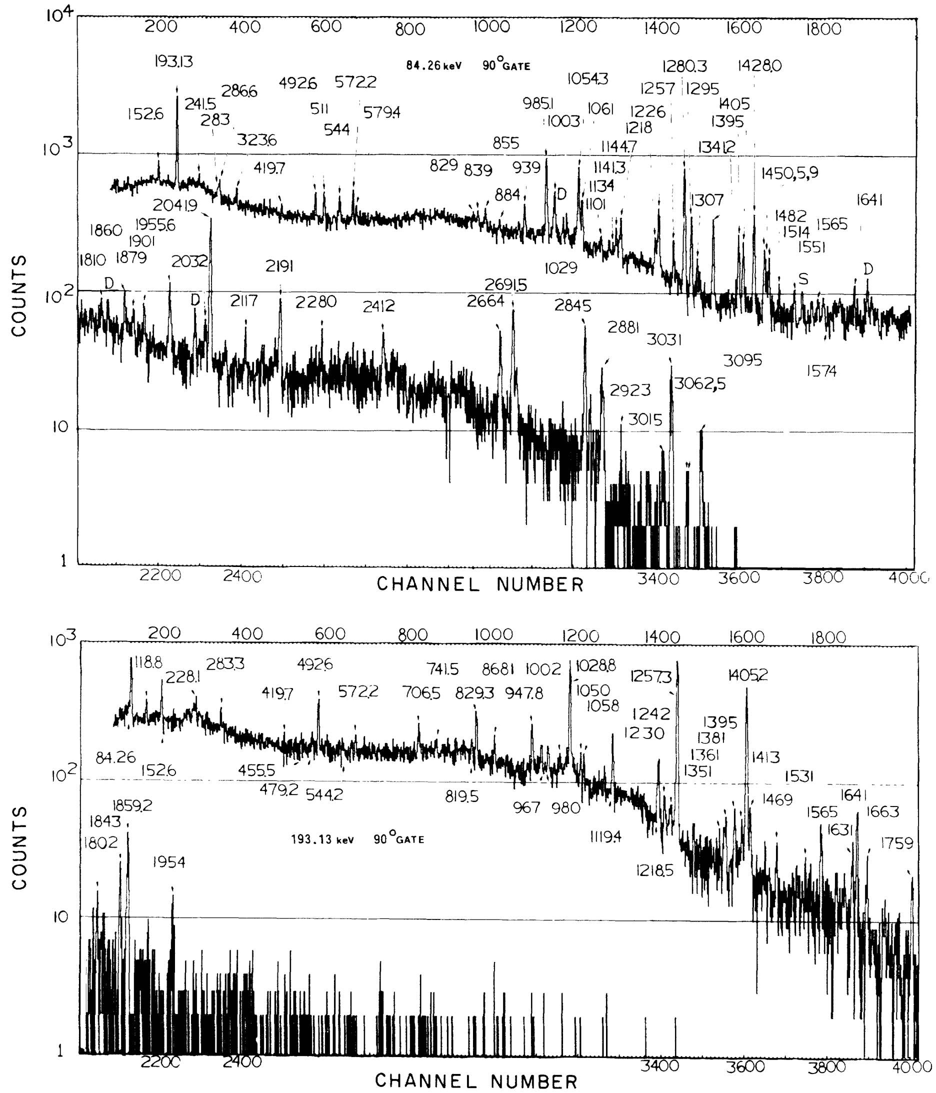

FIG. 6. Two examples of the more than 100 γ-γ coincidence spectra obtained. Shown here are 90° data for those γ rays in coincidence with the 84.26-keV 2+ to 0+ and the 193.13-keV 4+ to 2+ ground-band transitions. Many, but not all, of the γ rays identified in these two gates are labeled.

1364-keV $E1$ transitions to give the best average intensity normalization factor between the electron and the γ-ray data. The multipolarities of all but the 193-keV $E2$ transition were determined from decay systematics and from the directional correlation measurements by Paperiello *et al.*[10] It is worth noting that our low-energy conversion-electron intensity data (<400 keV) disagree significantly with the data given in Ref. 2.

D. Experimental Results

1. γ-Ray Energies and Intensities

The energies and intensities for the 550 γ-ray transitions observed in the decay of ^{170}Lu are listed in Table II. Also given are K conversion coefficients for the stronger lines obtained from the conversion-electron data, as well as data for eight $E0$ transitions. Where multipole assignments can be made they are listed as well.

For those transitions placed in the decay scheme (see Sec. IID3, below), assignment was based either on coincidence data or energy balance, denoted c.d. and e.b., respectively, in the last column of Table II. There were 212 γ-ray transitions assigned on the basis of coincidence data, and these account for 93% of the total γ-ray intensity observed. For these transitions, the initial and final energy levels are given, and wherever possible the spins and parities of the levels are also listed.

An additional 118 transitions have been assigned

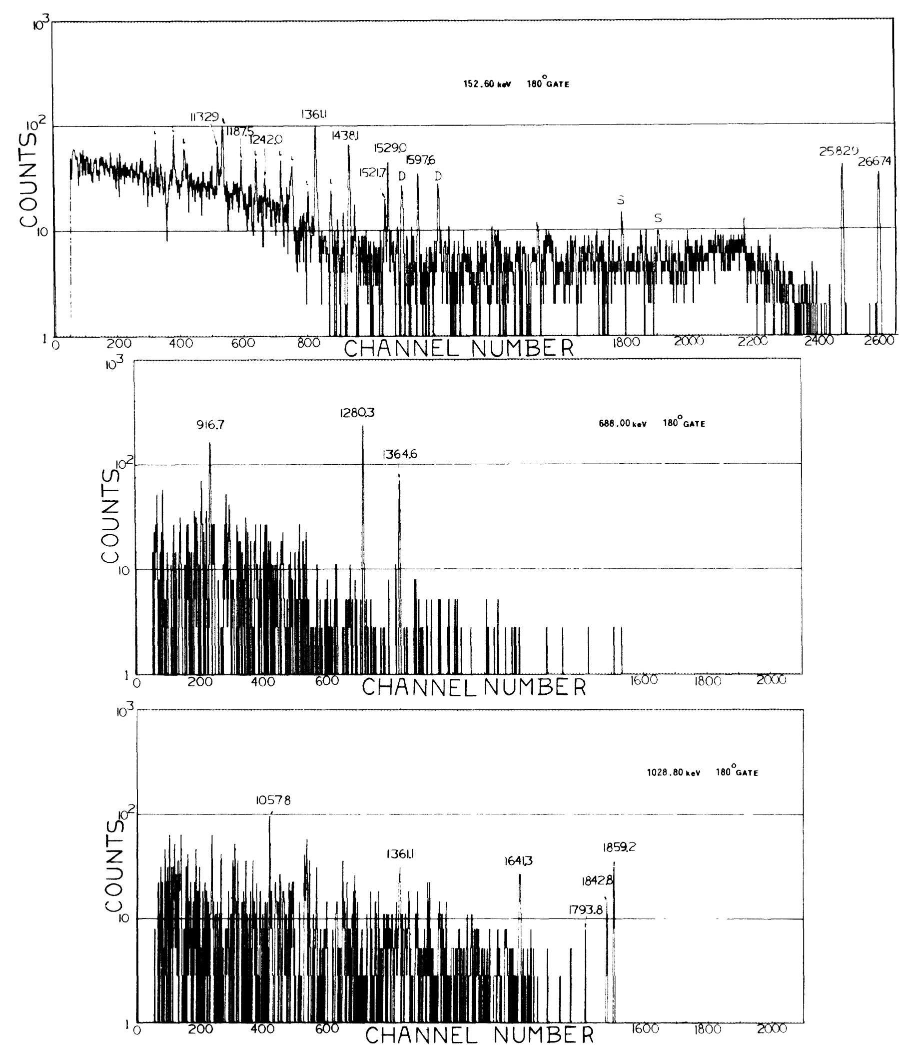

FIG. 7. Three examples of the forty 180° γ-γ coincidence gates sorted. Shown here are the 152.6-, 688.0-, and 1028.8-keV gates. A small i in the top spectrum identifies those transitions that are indirect, i.e., those that follow the labeled transitions. The S and D identify single- and double-escape peaks.

on the basis of energy balance, that is, agreement between the γ-ray transition energies and the level energy differences for those levels established by coincidence data. 13 transitions can be placed in either of two locations, and these choices are listed under the columns labeled E_i and E_f. Three transitions having three possible placements and one transition having four possible placements are indicated under E_i. These 118 transitions account for another 3% of the γ-ray intensity. Therefore, only 4% of the total observed intensity remains unassigned, and this small percentage involves the remaining 210 γ-ray transitions.

2. *Proposed ^{170}Yb Level Scheme*

The partial level scheme proposed for ^{170}Yb is shown in Figs. 9–12. The 61 levels shown are all based on γ-γ coincidence data. A few high-energy ground-state transitions whose energies agree very well with the established levels are also shown (those transitions lack the solid circles). The eight $E0$ transitions observed in the conversion-electron data are shown as dotted transitions. The 220 transitions shown account for 93% of the total observed γ-ray intensity. The electron-capture and positron branching to each level and the logft values have not been included in Figs. 9–12 but can be found in Table III. The bases for the spin, parity, and K quantum number assignments for each level are discussed in Sec. II D 4, below.

Once these 61 levels were established, it was possible to compare all of the energy level differences with the unassigned transitions. Those transitions agreeing with only one energy level difference were placed in another decay scheme, which is shown in Figs. 13 and 14. A total of 64 levels and 118 transitions is shown in this decay scheme.

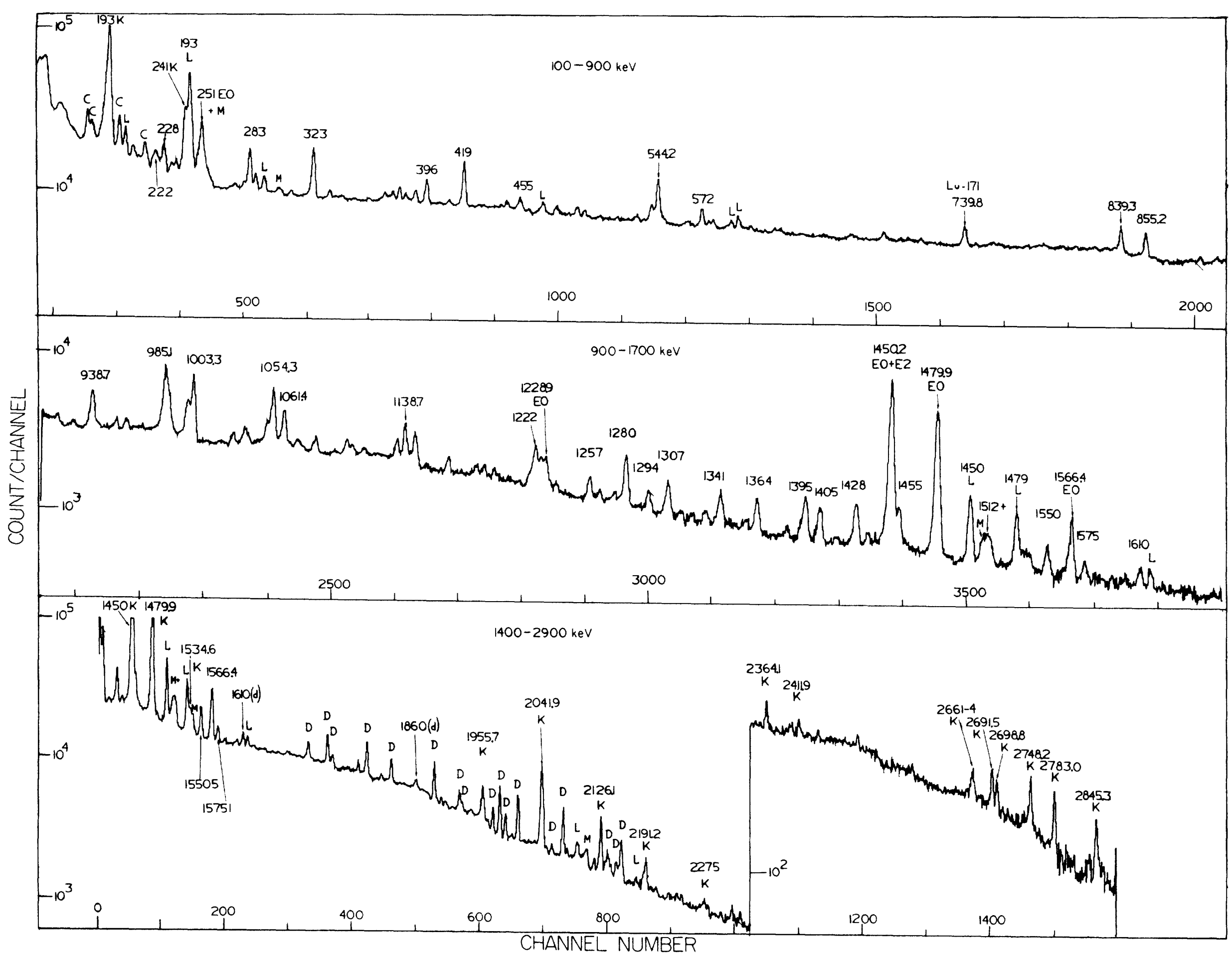

FIG. 8. A plot of the conversion-electron data obtained with a 3-mm depletion-depth Si(Li) detector. Contaminant activities are indicated by an upper-case C, while a lower-case d denotes a doublet and an upper-case D represents double-escape peaks from strong higher-energy transitions. Only some of the many conversion lines analyzed are identified.

TABLE II. γ-ray transitions, energies, intensities, multipolarities, and level assignments for all transitions observed in the decay of ^{170}Lu.

E_γ [a] (keV)	ΔE_γ [b] (keV)	I_γ [c] ($\% \times 10^3$)	ΔI_γ [d]	α_k [e] ($\times 10^{+4}$)	Multipolarity	$I_i\pi$ [f]	$I_f\pi$ [f]	E_i [g] (keV)	E_f [g] (keV)	Assignment via [h]
84.262	±0.004	195 000	±10 000		$E2$	2+	0+	84	0	c.d.
118.80	0.15	720	70			2−	2+	1425	1306	c.d.
119.90	0.20	150	15					2939	2819	e.b.
134.05	0.15	280	30					3099	2965	e.b.
142.50	0.15	210	20							
152.60	0.03	6100	200			0−	1−	2819	2667	c.d.
166.70	0.20	135	15					2367	2200	e.b.
170.80	0.20	70	10					3146	2975	e.b.
193.13	0.05	46 250	1500	1790	$E2$	4+	2+	277	84	c.d.
199.65	0.15	200	20							
201.75	0.15	350	30					1566	1364	e.b.
205.55	0.20	175	15					1717	1512	e.b.
209.90	0.20	165	15							
220.90	0.15	425	15	≤2100	$M1(E2)$	1−	1−	2496	2275	c.d.
222.40	0.15	900	30	2670	$M1(E2)$					
223.40	0.15	450	15	3320	$M1$					
225.45	0.20	130	20					2351	2126	e.b.
228.05	0.15	800	50	5420	$E0+E2$	2+	2+	1534	1306	c.d.
231.15	0.20	130	15					2768	2536	e.b.
235.55	0.15	880	80	1920	$M1E2$			2351	2116	e.b.
238.25	0.15	370	35					2667	2429	e.b.
241.50	0.05	5100	150	2380	$M1$	(0−)	1−	2367	2126	c.d.
249.95	0.20	85	25					2748	2498	e.b.
251.0	···	≤100	···	≥25 000	$E0$	0+	0+	1479	1228	e.b.
251.75	0.10	1050	50					2367	2116	e.b.
272.40	0.15	205	20					2939	2667	e.b.
275.40	0.20	100	10							
279.40	0.15	470	30					2775	2496	e.b.
283.05	0.10	4450	150	1240	$M1$	0−	1−	2819	2536	c.d.
286.60	0.05	10 100	300	180	$E1$	2−	2+	1425	1138	c.d.
292.55	0.20	110	10					1717	1425	e.b.
295.15	0.20	100	10					(4)		e.b.
296.70	0.20	170	15					(3)		e.b.
297.70	0.20	85	10							
300.60	0.20	100	10	2640	$M1$					
301.85	0.20	130	15 }	2050	{ $M1$			{ 2429	2126 }	
303.20	0.20	90	10 }					{ 2667	2364 }	
311.80	0.20	160	15					2351	2040	e.b.
323.57	0.05	7700	250	850	$M1$	0−	1−	2819	2496	c.d.
329.3	0.2	250	20			1−	1−	3149	2819	c.d.
337.5	···	≤100	···	≥1500	$E0$	0+	0+	1566	1228	e.b.
339.45	0.20	70	10					{ 2768 { 3115	2429 } 2775 }	
340.90	0.15	340	15							
366.35	0.15	540	20					{ 3149 { 2351	2783 } 1985 }	
368.30	0.20	200	10					2768	2400	e.b.
369.80	0.15	580	30							
371.90	0.15	680	40	<2100	$M1$	0−	1−	2498	2126	c.d.
374.55	0.20	100	10							
382.35	0.10	1300	50	<1300				2498	2116	e.b.
384.85	0.15	320	15							
386.45	0.20	200	15					3169	2783	e.b.
388.80	0.10	2000	60	600	$M1$	2+	2+	1534	1145	c.d.
390.40	0.15	1250	50							
395.95	0.10	4200	120	600	$M1$	2+	2+	1534	1138	c.d.

TABLE II *(Continued)*

E_γ [a] (keV)	ΔE_γ [b] (keV)	I_γ [c] ($\% \times 10^3$)	ΔI_γ [d]	α_k [e] ($\times 10^{+4}$)	Multipolarity	$I_i\,\pi$ [f]	$I_f\,\pi$ [f]	E_i [g] (keV)	E_f [g] (keV)	Assignment via [h]
401.30	0.20	190	60					3169	2768	e.b.
404.00	0.15	320	15	680	$M1$			{3179	2775}	
								{3065	2661}	
406.25	0.15	520	30							
407.55	0.20	200	10							
410.5	···	i	···}	≥2300	$E0$	0+	0+	1479	1069	e.b.
410.55	0.15	220	50}							
416.50	0.20	135	15					2768	2351	e.b.
419.65	0.05	11 200	300	430	$M1$	0−	1−	2819	2400	c.d.
427.20	0.20	190	30					3195	2768	e.b.
443.40	0.15	910	30	240	$M1E2$			(3)		e.b.
447.65	0.10	1575	50	475	$M1$					
449.25	0.20	160	15							
455.50	0.10	2900	100	≤465	$M1$	0−	1−	2819	2364	c.d.
457.90	0.15	480	40					2116	1658	e.b.
461.20	0.15	270	40	500	$M1$					
465.50	0.15	240	20							
467.35	0.15	490	25	475	$M1$			2965	2498	e.b.
472.50	0.15	250	10							
478.80	0.10	1250	140}	≤500				3146	2667	e.b.
479.50	0.15	670	30}					3140	2661	e.b.
480.50	0.15	440	20							
486.80	0.15	420	20							
490.95	0.15	500	15							
492.58	0.05	12 700	400}	56	$E1$	2−	3+	1717	1225	c.d.
497.0	···	i	···}	≥1400	$E0$	0+	0+	1566	1069	e.b.
497.50	0.15	310	10							
500.50	0.15	220	10					2929	2429	e.b.
518.90	0.15	220	10							
525.05	0.15	250	30							
530.50	0.10	2100	100	145	$E2$	0−	(2−)	2819	2289	c.d.
534.65	0.15	220	10}	210						
535.95	0.15	210	10}							
539.05	0.15	540	50							
540.15	0.10	4600	200	270	$M1$	0−	1−	2052	1512	c.d.
544.24	0.05	18 500	500	≤230	$M1$	0−	1−	2819	2275	c.d.
547.25	0.15	860	40					2748	2200	e.b.
558.90	0.15	350	35	80	$E1$					
560.55	0.15	370	50	325	$M1$					
563.00	0.15	960	30	≤210	$M1E2$					
565.80	0.15	280	15					3314	2748	e.b.
572.20	0.05	28 000	750	33	$E1$	2−	2+	1717	1145	c.d.
575.95	0.25	435	20	≤800	≤$M2$					
579.40	0.05	10 000	300	44	$E1$	2−	2+	1717	1138	c.d.
584.35	0.15	265	15							
585.80	0.15	340	20							
587.15	0.15	660	120	180	$M1E2$					
590.85	0.15	810	25							
595.70	0.15	700	20							
598.15	0.15	720	30							
612.15	0.15	930	30	78	$E2$			3149	2536	e.b.
614.00	0.20	200	10					2965	2351	e.b.
618.95	0.10	1650	50	110	$M1E2$			2819	2200	e.b.
621.40	0.15	970	100	230	$M1$					
622.75	0.20	550	35							
633.75	0.25	200	10					2351	1717	e.b.
636.80	0.20	500	80							
645.80	0.20	300	15							

TABLE II *(Continued)*

E_γ [a] (keV)	ΔE_γ [b] (keV)	I_γ [c] ($\% \times 10^3$)	ΔI_γ [d]	α_k [e] ($\times 10^{+4}$)	Multipolarity	$I_i \pi$ [f]	$I_f \pi$ [f]	E_i [g] (keV)	E_f [g] (keV)	Assignment via [h]
649.60	0.15	1000	60					{2775 {2367	2126} 1717}	
652.65	0.20	370	30							
655.10	0.20	225	10							
656.65	0.20	280	15					3179	2522	e.b.
658.20	0.20	220	15							
659.70	0.20	240	15					2775	2116	e.b.
670.35	0.20	840	40					3099	2429	e.b.
675.45	0.20	240	15					{2040 {2661	1364} 1985}	
681.50	0.25	175	10					3179	2498	e.b.
688.00	0.08	4400	150	150	$M1$	0−	1−	2052	1364	c.d.
691.75	0.20	370	15							
693.55	0.20	530	50					2819	2126	e.b.
700.15	0.20	465	15}	200	$M1$					
700.80	0.20	700	20}					2126	1425	e.b.
703.85	0.15	1700	50	160	$M1$			2819	2116	e.b.
706.50	0.45	1650	150}	27	$E1$					
707.10	0.15	3000	100}							
711.65	0.15	1600	50	190	$M1$			3140	2429	e.b.
723.05	0.20	440	20					2775	2052	e.b.
728.85	0.20	950	200					2929	2200	e.b.
741.50	0.20	970	30			1−		2400	1658	c.d.
746.90	0.20	680	20					2947	2200	e.b.
750.95	0.20	830	30					3115	2364	e.b.
756.15	0.20	450	20							
757.60	0.15	2550	100					3186	2429	e.b.
762.55	0.15	620	20					2748	1985	e.b.
785.75	0.20	620	70							
787.60	0.15	1200	80							
792.00	0.15	2350	120					3067	2275	e.b.
801.25	0.20	800	40							
802.40	0.20	730	35							
805.85	0.25	400	100							
809.25	0.20	620	30							
813.55	0.20	900	90					{2929 {2939	2116} 2126}	
815.70	0.20	520	25					{3179 {3314	2364} 2498}	
819.50	0.20	700	20			1−	2+	2126	1306	c.d.
822.30	0.15	2450	100							
829.30	0.10	10 850	300			1−	2+	2364	1534	c.d.
834.45	0.10	2230	75	30						
839.30	0.10	15 700	450	≤106	$M1$	0−	1−	2351	1512	c.d.
850.05	0.15	1050	50			1−	2−	2275	1425	c.d.
851.45	0.20	1800	100					2364	1512	e.b.
855.15	0.15	21 400	600	75	$M1$	(0−)	1−	2367	1512	c.d.
859.45	0.20	1300	100					2975	2116	e.b.
864.85	0.25	800	40					2522	1658	e.b.
868.10	0.20	1700	200			2+	4+	1145	277	c.d.
873.85	0.25	300	30					3149	2275	e.b.
876.80	0.25	600	30					2929	2052	e.b.
879.65	0.25	500	25							
884.10	0.15	7700	450			1−	0+	2364	1479	c.d.
895.00	0.25	540	30					2947	2052	e.b.
901.40	0.20	1500	70					{2040 {3169	1138} 2268}	
910.8	0.30	920	50			1−	1−	2275	1364	c.d.

TABLE II *(Continued)*

E_γ [a] (keV)	ΔE_γ [b] (keV)	I_γ [c] (% × 10^3)	ΔI_γ [d]	α_k [e] (× 10^{+4})	Multipolarity	$I_i\pi$ [f]	$I_f\pi$ [f]	E_i [g] (keV)	E_f [g] (keV)	Assignment via [h]
916.65		2200	200}	42		(2−)	1−	2429	1512	c.d.
916.90		1500	150}				0−	2969	2052	c.d.
926.40	0.15	5800	180	28	$E2$	0−	2−	2351	1425	c.d.
938.75	0.08	35 200	1000	68	$M1$	1−	2−	2364	1425	c.d.
942.45	0.15	4700	150			(0−)	2−	2367	1425	c.d.
947.80	0.15	3500	100			3+	4+	1225	277	c.d.
952.55	0.25	930	50							
954.30	0.15	5000	150	75	$M1$			2939	1985	e.b.
962.85	0.25	170	20							
966.85	0.20	3200	100					2364	1397	e.b.
969.05	0.20	1300	60					2275	1306	e.b.
970.20	0.20	2500	80					2116	1145	e.b.
980.30	0.20	2900	300	≤64		1−	2+	2126	1145	c.d.
983.67	0.20	7000	500			1−	1−	2496	1512	c.d.
985.10	0.10	120 000	4000	29	$E2$	0+	2+	1069	84	c.d.
987.25	0.10	37 000	1200	75	$M1$	0−	1−	2351	1364	c.d.
988.5	j	3000	300					2126	1138	c.d.
999.60	0.10	34 000	1000	56	$M1$	1−	1−	2364	1364	c.d.
1002.3	j	3000	300					2536	1534	c.d.
1003.20	0.10	77 000	2400	55	$M1$	(0−)	1−	2367	1364	c.d.
1009.50	0.30	880	50					2667	1658	e.b.
1012.30	0.30	290	30					3065	2052	e.b.
1028.80	0.10	18 000	600	31	$E2$	2+	4+	1306	277	c.d.
1034.20	0.30	600	200							
1046.60	0.25	1950	100					2275	1228	e.b.
1050.40	0.10	22 000	700	≤34	$M1E2$	(2−)	2−	2768	1717	c.d.
1053.7	i	2500	500}				1−	3179	2126	c.d.
1054.28	0.05	103 000	3300}	≤24	$E2$	2+	2+	1138	84	c.d.
1055.23	i	5000	1000}				2+	2200	1145	c.d.
1057.70	0.15	4750	150			1−	2+	2364	1306	c.d.
1060.58	0.20	5500	500				1−	3186	2126	c.d.
1061.35	i	5000	1000}			(0−)	2+	2367	1306	c.d.
1061.39	0.10	47 000	1500}	29	$E2$	2+	2+	1145	84	c.d.
1068.80	0.40	120	10}	≥2800						
1069.4	···	i	···}		$E0$	0+	0+	1069	0	e.b.
1070.90	0.30	1170	40			1−	2−	2496	1425	c.d.
1078.3	0.40	750	200					3131	2052	e.b.
1082.10	0.30	570	60							
1086.9	0.30	750	30							
1101.70	0.10	21 300	600	34	$E2$	0−	2−	2819	1717	c.d.
1110.65	0.30	270	15					2768	1658	e.b.
1113.10	0.20	2250	100	≤150		1−	2+	2748	1634	c.d.
1119.40	0.20	4000	120				4+	1397	277	c.d.
1122.5	0.30	350	10					2268	1145	e.b.
1124.65	0.30	850	25							
1132.86	j	1500	150}			1−	2+	2667	1534	c.d.
1133.60	0.10	23 000	750}	40	$M1$	0−	1−	2498	1364	c.d.
1135.1	j					1−	0+	2364	1228	c.d.
1137.05	0.30	3500	100			1−	2+	2275	1138	c.d.
1138.65	0.10	78 000	2400	24	$E2$	2+	0+	1138	0	c.d.
1141.30	0.20	11 400	350	22	$E2$	3+	2+	1225	84	
1144.65	0.20	37 200	1200	22	$E2$	0+	2+	1228	84	
1145.80	0.20	39 100	1500	23	$E2$	2+	0+	1145	0	
1155.25	0.30	750	50					(3)		
1158.45	0.30	460	25					{2522 {3274	1364} 2116}	
1162.35	0.30	900	50							

TABLE II *(Continued)*

E_γ [a] (keV)	ΔE_γ [b] (keV)	I_γ [c] ($\% \times 10^3$)	ΔI_γ [d]	α_k [e] ($\times 10^{+4}$)	Multipolarity	$I_i \pi$ [f]	$I_f \pi$ [f]	E_i [g] (keV)	E_f [g] (keV)	Assignment via [h]
1173.20	0.40	700	300			1−	1−	2536	1364	c.d.
1180.75	0.30	250	25							
1181.5	0.30	1000	200					2748	1566	e.b.
1187.50	0.30	1000	50			1−	0+	2667	1479	c.d.
1202.95	0.30	450	25							
1204.80	0.30	400	20							
1206.30	0.20	3000	150			1−	0+	2275	1069	c.d.
1211.20	0.30	800	40							
1213.65	0.20	1150	60					2748	1534	e.b.
1217.30	0.20	4500	150	30	$M1E2$					
1218.50	0.20	30 400	1000	6.5	$E1$	1−	2+	2364	1145	c.d.
1222.25	0.30	14 300	500	103	$E0+E2$	2+	2+	1306	84	c.d.
1225.65	0.10	108 000	3200	9.2	$E1$	1−	2+	2364	1138	c.d.
1228.9	···	k	···	≥500	$E0$	0+	0+	1228	0	e.b.
1230.20	0.30	2500	100	≤115		1−	2+	2536	1306	c.d.
1234.50	0.30	500	25					3274	2040	e.b.
1235.90	0.10	5100	150	50	$M1$	1−	1−	2748	1512	c.d.
1240.65	0.30	370	20							
1241.95	0.20	1100	50			1−	2−	2667	1425	c.d.
1257.20	0.10	30 500	1000	21	$E2$	2+	4+	1534	277	c.d.
1263.45	0.20	6900	200	45	$M1$	1−	1−	2775	1512	c.d.
1268.30	0.20	2600	100			1−	0+	2748	1479	c.d.
1280.25	0.10	177 000	5000	8.7	$E1$	1−	2+	1364	84	c.d.
1290.9	0.40	1900	350				2+	2429	1138	c.d.
1294.70	0.10	63 500	2000}	9.5	$E1$	1−	0+	2364	1069	c.d.
1294.74	j	1000	100}			1−	2+	2929	1634	c.d.
1304.85	0.20	2200	80			1−	2+	2939	1634	c.d.
1306.30	0.20	11 000	500	≤42	$E2$	2+	0+	1306	0	c.d.
1307.55	0.10	24 000	1000}	≤22	$M1$	0−	1−	2819	1512	c.d.
1307.97	j	2600	300}			1−	0+	2536	1228	c.d.
1312.90	0.30	7000	400				2+	1397	84	c.d.
1313.03	j	1000	100			1−	2+	2947	1634	c.d.
1323.00	0.20	3900	300			1−	2−	2748	1425	c.d.
1330.65	0.30	800	40					{2400	1069}	
								{2965	1634}	
1341.20	0.10	70 500	2000	9.5	$E1$	2−	2+	1425	84	c.d.
1350.45	0.30	1280	60			1−	2−	2775	1425	c.d.
1361.10	0.30	2500	250			1−	2+	2667	1306	c.d.
1364.60	0.10	100 000	···	7.9	$E1$	1−	0+	1364	0	c.d.
1370.40	0.30	520	25							
1373.50	0.20	3700	350					2939	1566	e.b.
1380.80	0.20	2700	350				4+	1658	277	c.d.
1383.60	0.20	4200	150			1−	1−	2748	1364	c.d.
1385.50	0.30	1000	50							
1395.03	j	9000	1000}			1−	2+	2929	1534	c.d.
1395.65	0.10	49 000	1500}	16	$E2$	0+	2+	1479	84	c.d.
1398.30	0.20	1500	300			1−	2+	2536	1138	c.d.
1403.79	i	4500	500			2−	1−	2768	1364	c.d.
1405.15	0.10	56 500	1800	≤11.6	$E1$	1−	2+	2939	1534	c.d.
1410.35	0.40	2850	300							
1413.20	0.20	4900	350			1−	2+	2947	1534	c.d.
1418.65	0.30	700	35					2783	1364	e.b.
1426.72	j	10 000	1000}			{1−	0+	2496	1069	c.d.
1427.27	j	7300	800}	9.1	$E1$	{1−	1−	2939	1512	c.d.
1428.08	0.10	75 500	2500}			{1−	2+	1512	84	c.d.
1435.40	0.20	5500	200			1−	1−	2947	1512	c.d.
1438.10	0.30	1100	50			1−	0+	2667	1228	c.d.

TABLE II *(Continued)*

E_γ [a] (keV)	ΔE_γ [b] (keV)	I_γ [c] (%×10^3)	ΔI_γ [d]	α_k [e] (×10^{+4})	Multipolarity	$I_i\pi$ [f]	$I_f\pi$ [f]	E_i [g] (keV)	E_f [g] (keV)	Assignment via [h]
1445.10	0.30	800	40							
1449.64	j	3000	400}	275		{1−	0+	2929	1479	c.d.
1450.20	0.10	35 000	1000}		$E0+E2$	{2+	2+	1534	84	c.d.
1455.25	0.10	25 500	750	≤25	$M1$	0−	1−	2819	1364	c.d.
1457.12	0.15	3800	400			(2−)	1−	2969	1512	c.d.
1459.85	0.10	23 500	750			1−	0+	2939	1479	c.d.
1463.25	0.30	1600	200					2975	1512	e.b.
1467.50	j	1500	150			1−	0+	2536	1069	c.d.
1467.93	j	2000	200			1−	0+	2947	1479	c.d.
1469.10	0.20	2000	100			1−	2+	2775	1306	c.d.
1479.9	···	≤200	···	≥32 600	$E0$	0+	0+	1479	0	e.b.
1482.15	0.10	13 500	500			0+	2+	1566	84	c.d.
1486.00	0.30	1000	50					2965	1479	e.b.
1490.45	0.30	530	30							
1498.75	0.30	760	40					3065	1566	e.b.
1503.85	0.40	200	20					2929	1425	e.b.
1507.80	0.20	1000	150	≤290			2+	3042	1534	c.d.
1512.50	0.10	55 300	1500	8.2	$E1$	1−	0+	1512	0	c.d.
1514.60	0.20	12 200	500	31	$M1$	1−	2−	2939	1425	c.d.
1518.85	0.30	1300	50					2748	1228	e.b.
1521.7	0.30	800	200			1−	2+	2667	1145	c.d.
1529.00	0.30	1600	150	39		1−	2+	2667	1138	c.d.
1531.30	0.20	4000	150	37	$M1$?	1−	2−	2956	1425	c.d.
1534.55	0.10	20 400	600	13.5	$E2$	2+	0+	1534	0	c.d.
1540.35	0.30	1900	100			1+	2−	2965	1425	c.d.
1549.92	j	2500	250			(0−)	2−	2975	1425	c.d.
1550.55	0.10	10 000	1 300	45	$E0+E2$	2+	2+	1634	84	c.d.
1560.25	0.30	285	25							
1564.97	j	2000	200			1−	1−	2929	1364	c.d.
1565.08	j	4500	200				2+	3099	1534	c.d.
1566.4	···	≤500	m ···	≥1660	$E0$	0+	0+	1566	0	e.b.
1573.60	0.25	2000	100				2+	1658	84	c.d.
1575.10	0.20	11 200	300	17	$M1$	1−	1−	2939	1364	c.d.
1583.30	0.30	1300	50			1−	1−	2947	1364	c.d.
1585.80	0.40	200	20							
1592.05	0.20	3100	100			1−	1−	2956	1364	c.d.
1597.55	0.30	1600	100			1−	0+	2667	1069	c.d.
1601.20	0.30	2600	100			1+	1−	2965	1364	c.d.
1602.20	0.30	2300	100			1−	2+	2748	1145	c.d.
1609.40	0.20	4800	250}	12	{$E1$	1−	2+	2748	1138	c.d.
1610.70	0.15	9600	500}		{$M1$	(0−)	1−	2975	1364	c.d.
1614.70	0.30	820	40					3149	1534	e.b.
1619.65	0.30	2000	100				0+	3099	1479	c.d.
1630.50	0.30	2200	50				2+	3165	1534	c.d.
1633.30	0.30	1150	200					2939	1306	e.b.
1634.80	0.30	2100	75	6.2	$E2$	2+	0+	1634	0	e.b.
1636.85	0.30	1200	40					3149	1512	e.b.
1641.30	0.20	6900	200			1−	2+	2947	1306	c.d.
1645.40	0.40	430	15					3179	1534	e.b.
1648.7	0.3	330	25							
1651.40	0.40	680	25					3131	1479	e.b.
1653.2	0.40	470	25					3165	1512	e.b.
1662.75	0.30	1425	75			(2−)	2+	2969	1306	c.d.
1667.10	0.40	690	35					3179	1512	e.b.
1674.20	0.30	3500	100				1−	3186	1512	c.d.
1678.60	0.20	5000	150			1−	0+	2748	1069	c.d.
1682.70	0.30	1200	400					3195	1512	e.b.

TABLE II *(Continued)*

E_γ [a] (keV)	ΔE_γ [b] (keV)	I_γ [c] ($\% \times 10^3$)	ΔI_γ [d]	α_k [e] ($\times 10^{+4}$)	Multipolarity	$I_i \pi$ [f]	$I_f \pi$ [f]	E_i [g] (keV)	E_f [g] (keV)	Assignment via [h]
1685.55	0.30	1300	150				0+	3165	1479	c.d.
1687.90	0.40	500	50							
1700.90	0.20	3000	100			1−	0+	2929	1228	c.d.
1703.30	0.30	1900	60							
1706.0	0.30	1050	150				2−	3131	1425	c.d.
1714.35	0.40	400	80					2939	1225	e.b.
1719.10	0.20	3250	100			1−	0+	2947	1228	c.d.
1723.75	0.30	600	40					{2947	1225}	
								3149	1425	
1731.30	0.40	210	20					2956	1225	e.b.
1736.60	0.30	870	120					2965	1228	e.b.
1740.65	0.30	1800	60				2−	3165	1425	c.d.
1746.30	0.30	675	35					2975	1228	e.b.
1747.75	0.40	250	25					3314	1566	e.b.
1753.85	0.30	1000	50							
1758.95	0.20	1800	60				2+	3065	1306	c.d.
1761.35	0.30	930	120					3186	1425	e.b.
1767.15	0.30	1800	100							
1770.35	0.40	250	25					3195	1425	e.b.
1776.10	0.30	5750	200				1−	3140	1364	c.d.
1778.80	0.40	540	50					3007	1228	e.b.
1783.30	0.40	540	50							
1784.70	0.40	880	150					3149	1364	e.b.
1791.70	0.4	780	20							
1793.75	0.3	2000	100				2+	3099	1306	c.d.
1796.30	0.5	400	20							
1799.25	0.5	285	20							
1802.25	0.15	3500	100			1−	2+	2947	1145	c.d.
1809.50	0.15	17 200	500	2.5	*E*1	1−	2+	2947	1138	c.d.
1818.75	0.45	470	45							
1820.65	0.45	350	35							
1824.60	0.45	680	65					3131	1306	e.b.
1830.10	0.45	430	40							
1832.40	0.40	530	20							
1836.65	0.45	1300	130					2975	1138	e.b.
1838.15	0.45	940	30					3067	1228	e.b.
1842.75	0.45	1150	70			1−	2+	3149	1306	c.d.
1843.30	0.30	2600	300							
1855.00	0.45	350	35							
1859.20	0.20	4500	700	8.7	*E*2		2+	3165	1306	c.d.
1860.30	0.15	12 100	500	3.6	*E*1	1−	0+	2929	1069	c.d.
1870.80	0.30	1300	150							
1874.75	0.45	610	30							
1876.15	0.30	3250	200							
1878.65	0.15	12 300	400			1−	0+	2947	1069	c.d.
1887.10	0.45	750	100							
1888.70	0.45	800	40							
1893.70	0.45	950	50							
1896.50	0.30	1230	60							
1901.35	0.15	13 200	500			2−	0+	1985	84	c.d.
1904.55	0.45	440	20							
1909.70	0.45	450	25							
1917.70	0.45	500	25							
1920.70	0.30	2100	75					3146	1225	e.b.
1936.90	0.30	4750	150				0+	3165	1228	c.d.
1954.00	0.30	3600	200	≤42			2+	3099	1145	c.d.
1955.65	0.15	29 800	1000	6.5	*E*2	1+	2+	2040	84	c.d.

TABLE II *(Continued)*

E_γ [a] (keV)	ΔE_γ [b] (keV)	I_γ [c] ($\% \times 10^3$)	ΔI_γ [d]	α_k [e] ($\times 10^{+4}$)	Multipolarity	$I_i\pi$ [f]	$I_f\pi$ [f]	E_i [g] (keV)	E_f [g] (keV)	Assignment via [h]
1960.80	0.30	6400	200				2+	3099	1138	c.d.
1962.45	0.30	2150	70							
1966.80	0.45	650	50					3195	1228	e.b.
1974.00	0.30	1200	40							
1977.40	0.45	700	150							
1983.90	0.45	570	30							
1985.50	0.30	1700	60					3131	1145	e.b.
1992.70	0.45	400	20					3131	1138	e.b.
1995.75	0.30	1800	70				0+	3065	1069	c.d.
1998.40	0.45	400	100							
2007.30	0.45	280	40					{3146	1138}	
								{3314	1306}	
2019.70	0.30	1350	100				2+	3165	1145	c.d.
2025.75	0.30	1250	50							
2027.20	0.30	3650	150				2+	3165	1138	c.d.
2030.15	0.20	6400	400				0+	3099	1069	c.d.
2031.70	0.20	8150	250			1−	2+	2116	84	c.d.
2040.00	0.15	56 800	2000	≥7.1	*M*1	1+	0+	2040	0	c.d.
2041.88	0.10	132 000	4000	3.0	*E*1	1−	2+	2126	84	c.d.
2046.5	0.5	580	30							
2054.35	0.3	2800	100							
2057.1	0.4	860	25					3195	1138	e.b.
2061.3	0.5	310	15					3131	1069	e.b.
2063.2	0.3	1580	50							
2086.4	0.5	450	20							
2094.5	0.5	615	30							
2096.3	0.2	3100	100			1−	0+	3165	1069	c.d.
2116.0	j	3500	400}	2.5	*E*1	1−	0+	2116	0	c.d.
2116.60	0.15	11 000	400}				2+	2200	84	c.d.
2126.11	0.10	111 000	3500	2.4	*E*1	1−	0+	2126	0	c.d.
2143.5	0.3	1600	60							
2148.5	0.5	750	25							
2152.9	0.5	430	20							
2157.7	0.5	220	10							
2165.7	0.5	290	15							
2178.0	0.5	420	20							
2183.9	0.5	880	50				2+	2268	84	c.d.
2191.15	0.15	35 500	1000	2.6	*E*1	1−	2+	2275	84	c.d.
2200.9	0.3	1200	50							
2205.3	0.4	760	30				2+	2289	84	c.d.
2223.9	0.5	350	40							
2232.7	0.5	350	15							
2243.7	0.4	720	50							
2246.8	0.5	250	15							
2255.4	0.6	175	15							
2257.4	0.4	700	25							
2266.8	0.5	360	20							
2268.15	0.30	4200	120				0+	2268	0	e.b.
2275.40	0.10	19 400	600	1.6	*E*1	1−	0+	2275	0	c.d.
2279.9	0.2	4250	150			1−	2+	2364	84	c.d.
2284.2	0.5	320	100							
2289.2	0.4	950	50				0+	2289	0	c.d.
2315.1	0.4	800	40							
2315.9	0.2	4600	150	5.1		1−	2+	2400	84	c.d.
2325.0	0.4	700	50							
2330.6	0.6	130	15							
2333.9	0.5	240	20							

TABLE II *(Continued)*

E_γ [a] (keV)	ΔE_γ [b] (keV)	I_γ [c] (% × 10^3)	ΔI_γ [d]	α_k [e] (× 10^{+4})	Multipolarity	$I_i\,\pi$ [f]	$I_f\,\pi$ [f]	E_i [g] (keV)	E_f [g] (keV)	Assignment via [h]
2344.9	0.5	1000	40				2+	2429	84	e.b.
2352.3	0.5	1100	40							
2364.10	0.15	32 400	1000	1.7	*E*1	1−	0+	2364	0	c.d.
2398.1	0.30	1000	200							
2400.15	0.20	9050	300	3.0	*E*1?	1−	0+	2400	0	c.d.
2411.90	0.15	17 900	600	1.6	*E*1	1−	2+	2496	84	c.d.
2419.9	0.50	430	70							
2424.4	0.30	2700	100							
2429.0	0.40	1050	100				0+	2429	0	e.b.
2438.6	0.30	2300	100	7.6	*M*1			2522	84	e.b.
2452.7	0.30	3000	100			1−	2+	2536	84	c.d.
2459.9	0.50	270	25							
2496.15	0.15	16 500	500	1.4	*E*1	1−	0+	2496	0	c.d.
2523.0	0.3	3000	100					2522	0	e.b.
2534.0	0.6	180	60							
2536.9	0.4	1400	100			1−	0+	2536	0	c.d.
2542.8	0.6	250	25							
2546.1	0.6	150	15							
2558.0	0.5	800	50							
2561.1	0.6	300	30							
2575.3	0.7	600	300							
2576.8	0.4	1700	300					2661	84	e.b.
2582.9	0.3	3100	100			1−	2+	2667	84	c.d.
2599.0	0.5	700	70							
2637.0	0.6	190	20							
2642.1	0.4	1900	100							
2652.0	0.4	450	50							
2653.0	0.6	800	80							
2661.0	0.30	5000	300	3.7	*M*1*E*2			2661	0	e.b.
2663.95	0.20	27 300	1000	1.4	*E*1	1−	2+	2748	84	c.d.
2667.4	0.5	1800	120	6.0	*M*1	1+	0+	2667	0	c.d.
2677.3	0.7	150	15							
2680.3	0.7	170	17							
2691.45	0.20	49 500	2000	1.1	*E*1	1−	2+	2775	84	c.d.
2698.80	0.30	13 200	500	3.2	*M*1*E*2	1+	2+	2783	84	c.d.
2718.3	0.6	350	35							
2720.9	0.5	950	50							
2726.6	0.6	250	25							
2729.3	0.7	200	20							
2735.6	0.6	550	50					2819	84	e.b.
2737.2	0.4	1250	200							
2748.15	0.20	46 300	2000	1.5	*E*1	1−	0+	2748	0	e.b.
2775.7	0.3	2450	100							
2783.00	0.20	22 400	1000	3.2	*M*1	1+	0+	2783	0	e.b.
2793.1	0.7	260	25							
2805.0	0.6	650	25							
2813.7	0.6	450	50							
2845.30	0.20	37 200	2000	1.4	*E*1	1−	2+	2929	84	c.d.
2849.5	0.30	4600	400	2.7	*E*2					
2855.4	0.30	7100	300	1.4	*E*1	1−	2+	2939	84	c.d.
2863.6	0.30	2870	100			1−	2+	2947	84	c.d.
2872.5	0.40	1680	80			1−	0+	2956	0	c.d.
2881.40	0.20	16 300	750			1+	2+	2965	84	c.d.
2885.1	0.30	6500	250			(2−)	2+	2969	84	c.d.
2897.6	0.50	1000	70							
2923.3	0.3	4000	200				2+	3007	84	c.d.
2929.50	0.20	13 000	650			1−	0+	2929	0	e.b.

TABLE II *(Continued)*

E_γ [a] (keV)	ΔE_γ [b] (keV)	I_γ [c] ($\% \times 10^3$)	ΔI_γ [d]	α_k [e] ($\times 10^{+4}$)	Multipolarity	$I_i \pi$ [f]	$I_f \pi$ [f]	E_i [g] (keV)	E_f [g] (keV)	Assignment via [h]
2939.65	0.20	33 500	2000			1−	0+	2939	0	e.b.
2947.80	0.20	12 900	650			1−	0+	2947	0	e.b.
2953.1	0.5	750	150							
2956.6	0.4	1900	60				0+	2956	0	e.b.
2958.1	0.4	1000	50				2+	3042	84	c.d.
2965.6	0.20	27 900	1500				0+	2965	0	e.b.
2969.7	0.5	600	70							
2981.5	0.5	700	70							
2983.1	0.4	1700	100				2+	3067	84	c.d.
2985.9	0.4	1200	80							
3007.5	0.3	3050	150				0+	3007	0	e.b.
3015.10	0.3	5500	250				2+	3099	84	c.d.
3018.5	0.6	320	30							
3030.95	0.20	28 600	1500			1−	2+	3115	84	c.d.
3036.90	0.3	4600	200							
3042.8	0.4	1500	75				0+	3042	0	e.b.
3046.9	0.5	750	75				2+	3131	84	e.b.
3053.1	0.3	2400	200							
3062.1	0.3	2300	200					3146	84	e.b.
3064.8	0.3	5600	250			1−	2+	3149	84	c.d.
3067.0	0.3	2600	200				0+	3067	0	e.b.
3085.4	0.6	330	20					3169	84	e.b.
3091.9	0.3	3400	200							
3095.50	0.20	7200	400				2+	3179	84	c.d.
3099.55	0.25	4300	250				0+	3099	0	e.b.
3102.1	0.6	330	30					3186	84	e.b.
3111.5	0.3	3900	200			1−	2+	3195	84	c.d.
3115.20	0.25	16 200	800			1−	0+	3115	0	e.b.
3119.2	0.6	450	150							
3123.0	0.6	420	40							
3128.1	0.5	900	90							
3130.9	0.7	250	40				0+	3131	0	e.b.
3139.6	0.8	65	15							
3146.1	0.4	2500	200					3146	0	e.b.
3149.4	0.4	2250	200			1−	0+	3149	0	e.b.
3157.0	0.8	90	10							
3161.1	0.5	1000	100							
3165.3	0.4	2200	200					3165	0	e.b.
3169.6	0.8	100	15					3169	0	e.b.
3173.4	0.7	300	30							
3179.8	0.7	375	40							
3183.6	0.5	1400	140							
3190.3	0.5	1250	120					3274	84	e.b.
3195.3	0.4	2000	200					3195	0	e.b.
3202.4	0.5	1500	150							
3206.8	0.8	300	30							
3212.2	0.8	150	15							
3218.4	0.9	50	10					3302	84	e.b.
3229.5	0.8	150	15					3314	84	e.b.
3255.9	0.7	300	30							
3258.2	0.8	250	25							
3274.2	0.5	1000	100					3274	0	e.b.
3282.1	0.8	50	10							
3291.4	0.7	100	10							

TABLE II (*Continued*)

E_γ [a] (keV)	ΔE_γ [b] (keV)	I_γ [c] (%×10³)	ΔI_γ [d]	α_k [e] (×10⁺⁴)	Multipolarity	$I_i\pi$ [f]	$I_f\pi$ [f]	E_i [g] (keV)	E_f [g] (keV)	Assignment via [h]
3302.4	0.7	260	25					3302	0	e.b.
3314.1	0.7	280	30					3314	0	e.b.
3338.9	0.8	40	10							
3385.0	0.8	40	10							

[a] The γ-ray energies have been rounded off in most cases to the nearest multiple of 50 eV.

[b] The final energy errors are adopted on the basis of the strength and multiplicity of the γ rays. For the strongest transitions the errors range from ±50 eV at low energy to ±250 eV above 3.1 MeV, while the weakest transitions have been assigned errors from ±200 eV at low energy to ±1.0 keV above 3.1 MeV.

[c] See text for a discussion of the method of intensity determinations. The 1364.6-keV transition intensity was adopted as 100 000 units (100%×10³).

[d] The intensity errors have the same units (%×10³) and include both the error in the Ge(Li) detector efficiency curve (±5% < 100 keV; ±3% 100 keV to 2.5 MeV; ±5% ≤ 3.1 MeV; and ±10% > 3.1 MeV) and the systematic error arising from differing results from different runs.

[e] Those conversion coefficients preceded by a ≤ sign indicate that the conversion line contained additional strong components from either ^{169}Lu or ^{171}Lu impurities or ^{170}Lu *L* or *M* conversion lines from strong ^{170}Lu transitions.

[f] No spin and parity information is entered unless the transition is believed to be firmly placed – i.e., appears on the coincidence γ-ray decay scheme.

[g] Initial and final excited state energies are given to aid in identifying placement. Where two possibilities exist, both are shown, otherwise the number of possible placements appears in parentheses (n).

[h] The level assignments are based either on γ-γ coincidence data denoted c.d. or on energy differences or energy balance denoted e.b.

[i] In calculating the lower limit to α_K, the intensity of any γ-ray observed at that energy is assumed.

[j] An unresolved multiplet; energies and intensities are determined from the level scheme and coincidence data, respectively.

[k] The nearby intense 1225.65-keV γ ray sets the upper limit for an observable 1228.9-keV γ ray at 2000 units, thus the low α_K limit.

[l] This line may be a doublet.

[m] A doublet at 1565 keV sets the observable intensity for a 1566.4-keV transition at 5000 units, thus the α_K limit.

Many of the transitions shown are undoubtedly correctly assigned; however, a few may be misassigned because they really belong to one or several "unknown" levels not shown in either Figs. 9–12 or 13 and 14. An indication of the small percentage of incorrect assignments is given by those 17 transitions mentioned earlier that have either two, three, or four possible placements. These transitions represent only 5% of the 328 transitions not assigned on the basis of coincidence data. The 118 transitions placed in Figs. 13 and 14 were included in the calculation of the intensity balances and log*ft* values.

The position of the 6+ ground-rotational-band member was calculated with the formalism outlined by Mariscotti, Scharff-Goldhaber, and Buck.[22] The 6+ level is shown as a tentative (dashed) level in Figs. 13 and 14 at an energy of 572.3 keV. The 0.3-keV error in this level is based on the 4-eV error in the 2+→ 0+ transition and the 50-eV error in the 4+→ 2+ ground-band transitions. This is easily in agreement with the value observed in (*d, t*) and (*d, d'*) experiments reported by Burke and Elbek.[23]

The ^{170}Yb level scheme is so complex that a detailed discussion of differences between this work and that of Bonch-Osmolovskaya *et al.*[12] is not practical. Instead, only a few of the major differences are noted here. We do not see levels at 1757.6, 2113.2, 2533.1, 2883.6, and 3091.9 keV. A majority of the transitions issuing from these levels are placed elsewhere in our decay scheme by coincidence data. A comparison of transitions in the decay scheme of Ref. 12 and those in our Table II is relatively easy and will show which assignments differ. The 2521.3-keV level of Ref. 12 resembles our 2523.0-keV level only in the two transitions to the 2+0 and 0+0 levels of the ground band. Two additional transitions assigned to the 2523-keV level in Ref. 12 are placed elsewhere by our coincidence data. The 2641.4-keV level proposed in Ref. 12 may exist. We observe two transitions at 2642.1 and 2558.0 keV that suggest a level at 2642.2 keV but such energy couplets seem too numerous to assign levels on that basis without additional supporting evidence. The 884.1-keV transition proposed in Ref. 12 to deexcite this level is placed elsewhere by our coincidence data. The proposed 3148.3-keV level may correspond to the two levels at 3146.2 and 3149.2 keV established by our coincidence data.

Several transitions issuing from these levels decay to the same level in both schemes, but the transition energies differ. The 3301.7-keV level of Ref. 12 may correspond to our 3302.6-keV level. Again, the ground-band transitions are placed by both Ref. 12 and by us, but with different energies. One of their transitions is placed elsewhere by our coincidence data, and two fit elsewhere by energy balance. Numerous other levels not discussed here have many associated transitions that are assigned differently in our level scheme on the basis of coincidence data.

3. *EC-β^+ Decay, Logft's, and Q Value of ^{170}Lu*

Table III lists a summary of the electron-capture plus positron branching ratios and associated information for 70 excited states in ^{170}Yb. The second column lists the net γ-ray intensity out of each level in units that are 10^{-3} of the transition intensity units given in Table II. In some cases, a positive or negative balance occurs that is consistent with zero net feeding within the errors of the intensity balance. These cases are indicated by parentheses around the percentage of electron capture plus positron decay in column three of Table III.

The spin and parity of ^{170}Lu is 0+, and Hansen *et al.*[9] measured positron feeding to the ^{170}Yb ground state as $0.19 \pm 0.05\%$ with an end-point energy of 2390 ± 50 keV. Thus, a Q value of 3410 keV was adopted for the total available decay energy, and 99.36% was assumed to be the total EC + β^+ feeding to the excited states of ^{170}Yb. The logft values in column four are derived from a nomogram[24] and assume a ^{170}Lu half-life of 51.8 h.[10] The spin, parity, and K quantum number assignments are listed in column five.

4. *Spin and Parity Assignments*

The data on which we base spin-parity assignments for levels in ^{170}Yb are primarily K conversion coefficients, logft's, and γ-ray branching ratios, although the angular-correlation data of Paperiello *et al.*[10] provide direct confirmation for a few of the assignments. The discussion of spin-parity assignments is divided into two parts, since a rather natural division is apparent in the ^{170}Yb level scheme. Most of the spin-two and spin-three states populated in the ^{170}Lu decay occur below the obvious gap in the level structure at 1800 keV. In fact, only one state with a probable spin greater than 1 is identified above this gap. Below the gap lie several states that would normally be considered to have substantial collective character. This lower group of states is considered first. No attempt is made to discuss each case of disagreement between our spin assignments and those given by Bonch-Osmolovskaya[12] and Mihelich.[13] In Table IV, our spin-parity assignments and those from these latter two references are summarized.

1069.4-, 1138.6-, 1145.6-, and 1224.5-keV levels. The level at 1069.4 keV is assigned $I\pi K = 0{+}0$ (see also Ref. 23) primarily on the basis of a conversion-electron line corresponding to an $E0$ transition from that energy level to ground. The $E2$ character of the 985.1-keV $0{+}0 \to 2{+}0_0$ transition is confirmed both by conversion-coefficient data and by the angular-correlation data of Paperiello *et al.*[10]

Energy spacing and other available decay data suggest that either the 1138.6- or 1145.6-keV state may be the 2+ member of this first excited 0+ band. Neither state displays the relative strength in the $E2$ branch to the $4{+}0_0$ ground-band member that would distinguish it as $K=0$ according to vector-coupling rules. Moreover, the $E0$ strength from the 0+ band head at 1069.4-keV to ground is very small (cf. Table II), so that no enhancement of the 1054.3- or 1061.4-keV conversion coefficients is expected or measured.

The (d, d'), and (d, t) data of Burke and Elbek[23] suggest a solution to this problem. Though the absolute energy uncertainties in their data are substantial (5–10 keV), the relative energies can be normalized to those precisely known from decay work, and the conclusion that the 1138.6-keV state is the ^{170}Yb γ vibration seems fairly certain. On that basis then, and from elementary theoretical expectations, the $K=0$ assignment for the 1145.6-keV state is virtually required, and this state is then assigned as the 2+ rotation based on the 1069.4-keV 0+ state.

The first rotational excitation based on the γ vibrational state is also observed at 1225.4 keV. The branching ratio to the 2+ and 4+ ground-band members, and the dominant $E2$ character of the 1141.3-keV $3{+} \to 2{+}$ transition, both support the 3+2 assignment for this state.

1228.9- and 1306.4-keV states. The 1228.9- and 1306.4-keV levels form the second excited 0+ "band" to be observed in ^{170}Yb. The $0{+}0_2$ state is clearly indicated by the K conversion-electron line corresponding to an $E0$ transition of 1228.9 keV, and in this case, the $E0$-enhanced conversion coefficient of the $2{+} \to 2{+}$ transition at 1222.2 keV, together with the close agreement of branching into the ground band with Alaga's rules, leaves little doubt that the assignment for the 1306.4-keV state is 2+0.

1364.6- and 1397.0-keV states. At 1364.6 keV is encountered the first of many 1-0 states observed in the ^{170}Yb level structure. Branching from this state into the ground band favors the 2+ state by the 2:1 reduced intensity ratio expected for a $K=0$

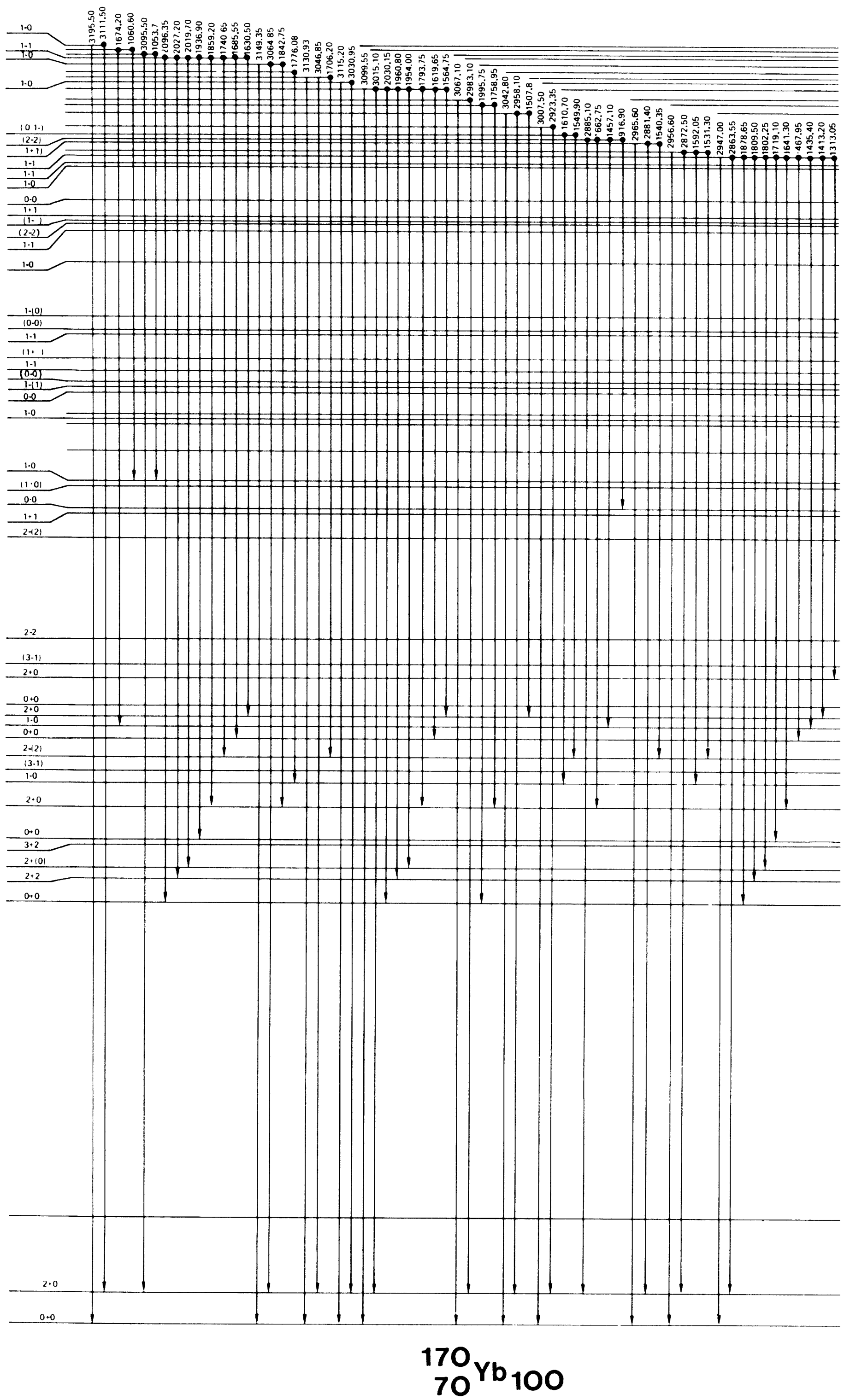

FIG. 9. A partial level scheme for ^{170}Lu, showing only those levels and transitions firmly established from coincidence data. See Table II for EC branching ratios and log*ft* values.

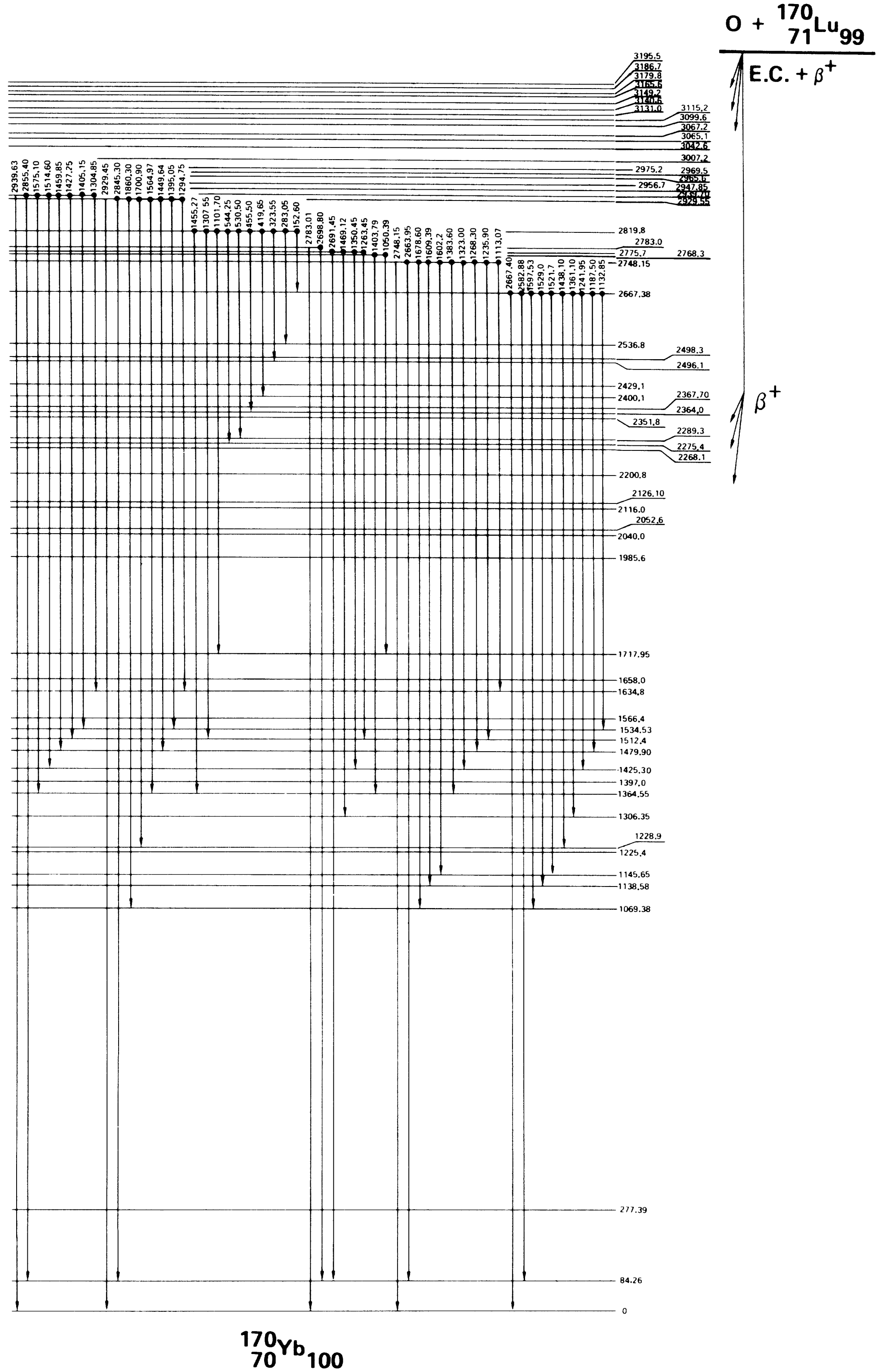

FIG. 10. A partial level scheme for ^{170}Lu, showing only those levels and transitions firmly established from coincidence data. See Table II for EC branching ratios and log*ft* values.

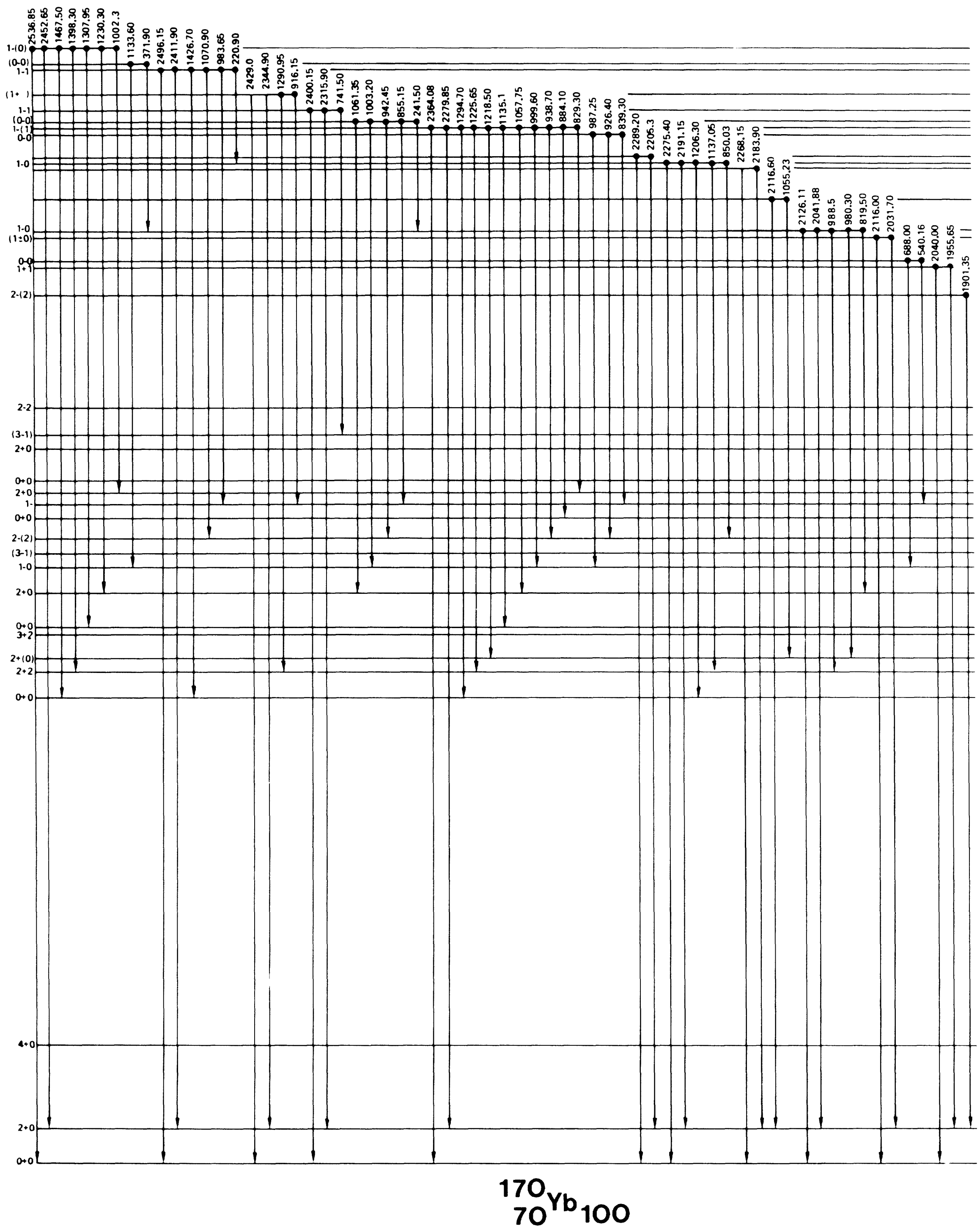

FIG. 11. A partial level scheme for ^{170}Lu, showing only those levels and transitions firmly established from coincidence data. See Table II for EC branching ratios and logft values.

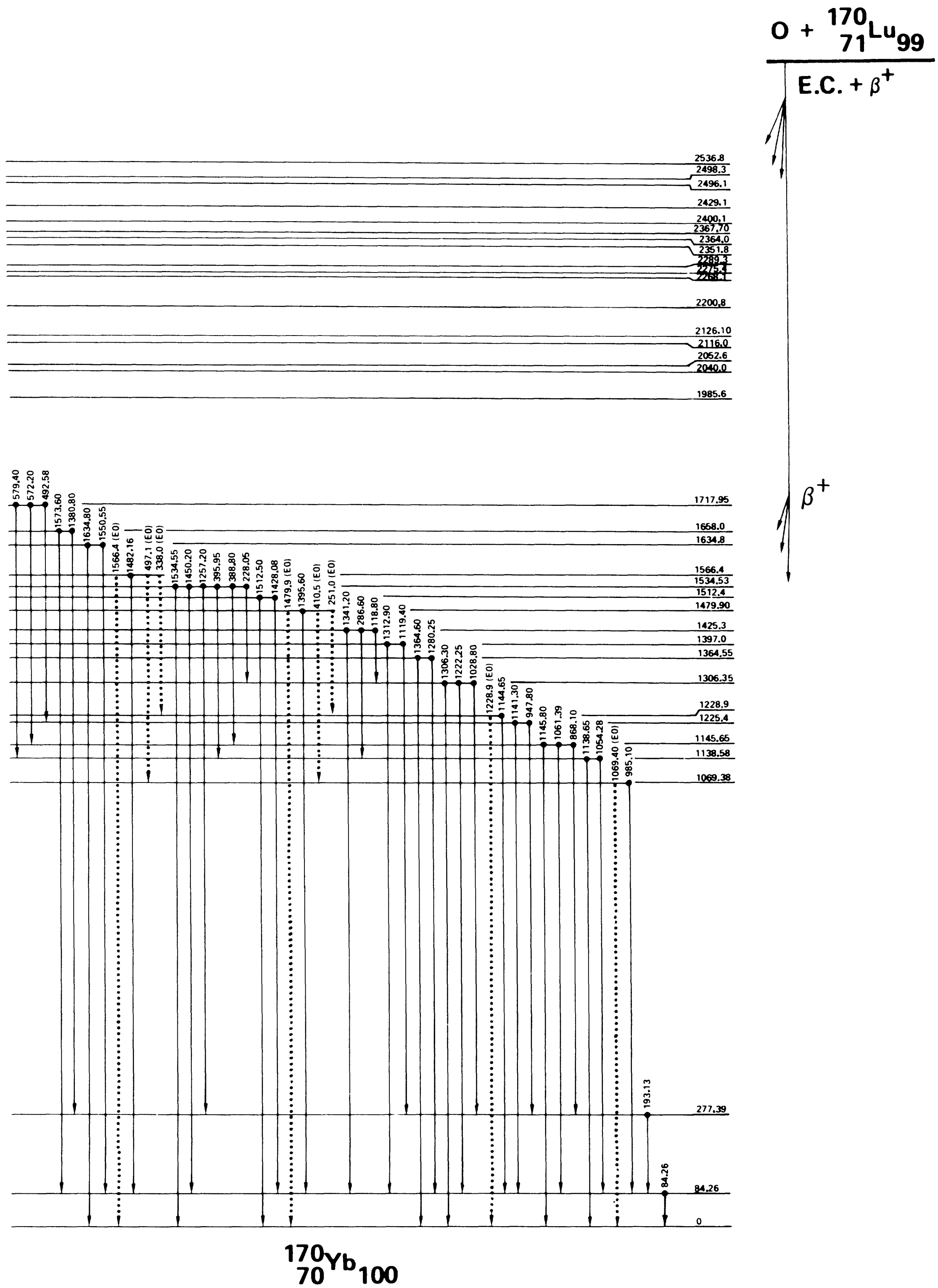

FIG. 12. A partial level scheme for ^{170}Lu, showing only those levels and transitions firmly established from coincidence data. The eight $E0$ transitions observed are indicated by "dotted" lines. See Table II for EC branching ratios and logft values.

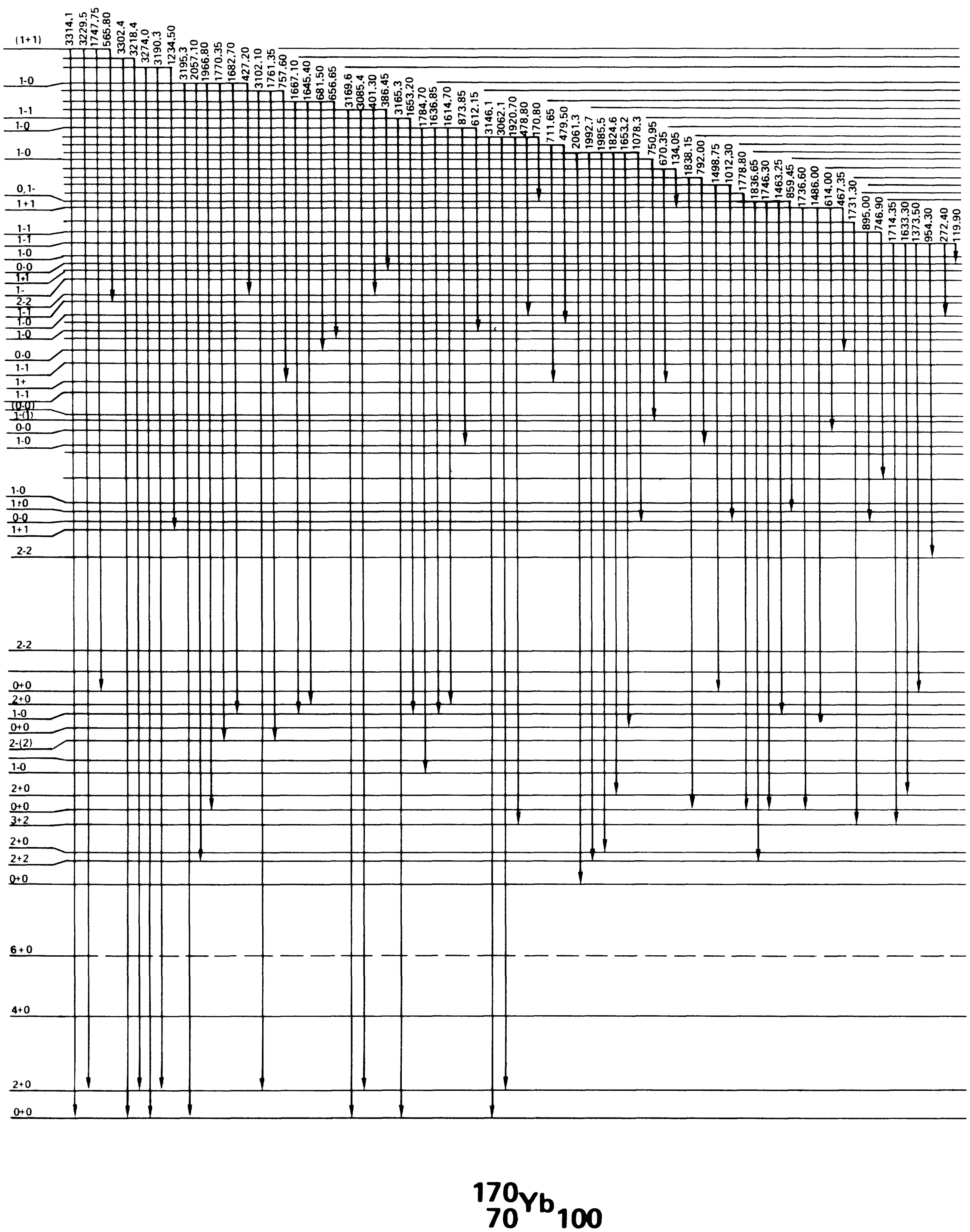

FIG. 13. A partial level scheme of ^{170}Lu, showing additional transitions that were placed on the basis of energy sums and differences alone.

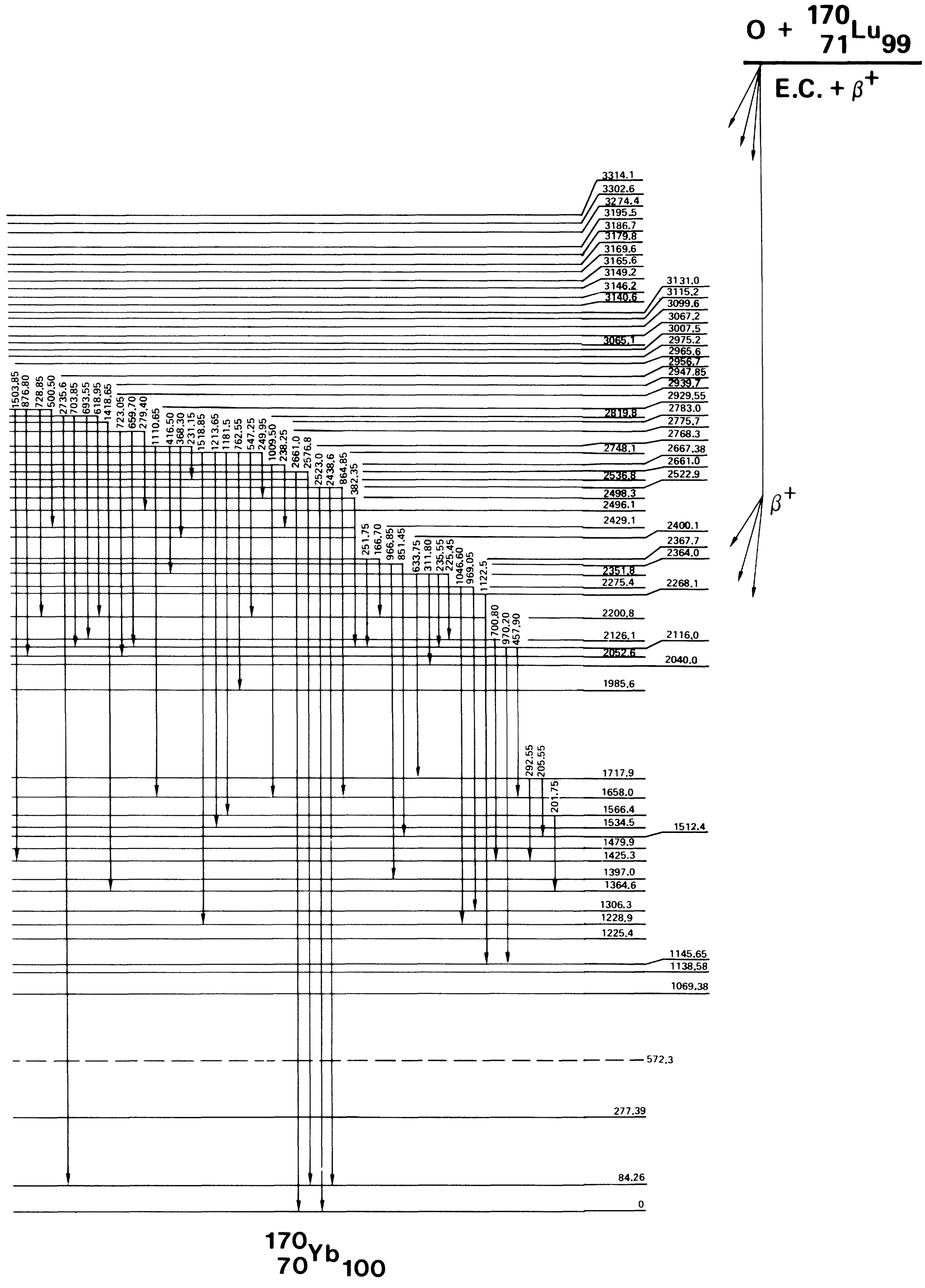

FIG. 14. A partial level scheme of ^{170}Lu, showing additional transitions that were placed on the basis of energy sums and differences alone.

state. Conversion data indicate $E1$ multipolarity for both the 1280- and 1364-keV γ rays. Angular-correlation data from the work of Paperiello *et al.*[10] further support the 1-0 assignment for this level.

The level at 1397 keV may be the spin-three member of this lowest 1-0 band, but we are unable to confirm such an assignment. The energy spacing (32 keV) seems far too small, though such bands can be strongly perturbed; if indeed the $\log ft$ is 9.3, then the spin-three assignment itself seems in doubt.

1425.3-keV state. The 286.6- and 1341.2-keV transitions out of the 1425.3-keV state are both identified as $E1$ from K conversion coefficients. The absence of a 199.9-keV branch to the 3+2 state at 1225.4 keV is puzzling (perhaps the 199.65-keV transition belongs here). If K is 2 for the 1425-keV state, one expects substantial feeding to both the spin-three and spin-two members of the low-lying $K=2+$ band. Instead, only the $2 \rightarrow 2$ branch occurs. Similarly, the absence of branches to other than the 2+ ground-band members seems to limit the spin to two.

1479.9- and 1534.5-keV states. The 1479.9- and 1534.5-keV levels are the 0+ and 2+ band members of the third $K=0+$ excitation. The 1479.9-, 410.5-, and 251.0-keV $E0$'s provide positive identification of the 1479.9-keV level as 0+, and the K conversion coefficient data for transitions from the 1534.5-keV state, together with γ-ray branching ratios for transitions into the ground band, provide the necessary information for the $2{+}0_3$ assignment at 1534.5 keV.

1512.4-keV state. The $E1$ character of the 1512.5- and 1428.1-keV transitions to the ground band, and their approximate 1 : 2 reduced intensity

TABLE III. Net γ-ray intensity out, total EC $+\beta^+$ feeding, $\log ft$ values, and $I\pi K$'s of all levels proposed in ^{170}Yb.

Level (keV)	$(0-I)$ $\times 10^{-3}$	%(EC $+\beta^+$)	$\log ft$	$I\pi K$
0		0.64	9.72	0+0
84.262 ± 0.004	23 ± 70	(1.08 ± 3.34)	>10	2+0
277.39 ± 0.03	−0.4 ± 2.4	(0.02 ± 0.11)	>11	4+0
572.28		0	>12	6+0
1069.40 ± 0.05	−0.7 ± 6.0	(0.03 ± 0.25)	>9.6	0+0
1138.58 ± 0.03	5.6 ± 8.2	(0.27 ± 0.39)	>9.6	2+2
1145.65 ± 0.05	4.2 ± 5.0	(0.20 ± 0.24)	>9.7	2+0
1225.4 ± 0.10	−0.5 ± 0.6	(0.02 ± 0.03)	>10.6	3+2
1228.9 ± 0.1	14.0 ± 1.7	0.67 ± 0.08	9.11	0+0
1306.35 ± 0.10	3.4 ± 3.6	(0.16 ± 0.17)	>9.7	2+0
1364.55 ± 0.05	28.0 ± 10.0	1.33 ± 0.48	8.77	1−0
1397.0 ± 0.2	7.8 ± 0.6	0.37 ± 0.03	9.32	
1425.30 ± 0.10	2.3 ± 4.0	0.11 ± 0.19	≥9.8	2−2
1479.90 ± 0.10	4.4 ± 2.6	0.21 ± 0.12	9.55	0+0
1512.4 ± 0.10	16.0 ± 7.0	0.75 ± 0.33	8.98	1−0
1534.53 ± 0.05	1.0 ± 5.0	(0.05 ± 0.24)	>10.1	2+0
1566.4 ± 0.1	8.3 ± 0.8	0.40 ± 0.04	9.23	0+0
1634.8 ± 0.1	5.7 ± 0.9	0.27 ± 0.04	9.36	2+0
1658.0 ± 0.1	1.3 ± 0.5	0.06 ± 0.02	10.0	
1717.95 ± 0.05	7.5 ± 2.0	0.36 ± 0.09	9.19	2−2
1985.6 ± 0.1	7.6 ± 0.6	0.36 ± 0.03	9.05	2−(2)
2040.0 ± 0.05	86.4 ± 3.0	4.09 ± 0.14	7.95	1+1
2052.6 ± 0.05	6.4 ± 0.4	0.31 ± 0.02	9.07	0−0
2116.0 ± 0.10	8.2 ± 0.9	0.39 ± 0.04	8.94	1−0
2126.10 ± 0.05	233.0 ± 8.0	11.04 ± 0.38	7.47	1−0
2200.8 ± 0.1	11.7 ± 1.5	0.56 ± 0.07	8.71	
2268.1 ± 0.1	5.4 ± 0.2	0.26 ± 0.01	9.00	
2275.4 ± 0.1	44.1 ± 2.2	2.08 ± 0.10	8.09	1−0
2289.3 ± 0	−0.4 ± 0.3	0.02 ± 0.01	>10	
2351.8 ± 0.05	62.5 ± 2.0	2.96 ± 0.09	7.66	0−0
2364.05 ± 0.05	332.3 ± 10.5	15.75 ± 0.50	7.13	1−(1)
2367.70 ± 0.05	117.4 ± 4.4	5.56 ± 0.20	7.50	(0−0)
2400.15 ± 0.10	3.2 ± 0.6	0.15 ± 0.03	9.11	1−1
2429.1 ± 0.1	0.8 ± 0.8	(0.04 ± 0.04)	>9.7	
2496.15 ± 0.10	44.4 ± 2.7	2.10 ± 0.13	7.86	1−1
2498.3 ± 0.1	24.3 ± 0.9	1.15 ± 0.04	8.13	(0−0)
2522.9 ± 0.1	5.8 ± 0.3	0.28 ± 0.01	8.72	(1+)
2536.8 ± 0.1	7.0 ± 1.1	0.33 ± 0.05	8.64	1−(0)
2661.0 ± 0.1	6.0 ± 0.6	0.29 ± 0.03	8.57	
2667.38 ± 0.05	9.0 ± 1.1	0.43 ± 0.05	8.38	1−0
2748.15 ± 0.05	108.5 ± 4.7	5.14 ± 0.22	7.21	1−1
2768.3 ± 0.2	26.9 ± 1.2	1.27 ± 0.06	7.79	(2−2)
2775.7 ± 0.1	60.8 ± 2.4	2.88 ± 0.11	7.43	1−
2783.0 ± 0.2	36.1 ± 1.5	1.71 ± 0.07	7.64	1+1
2819.80 ± 0.10	128.0 ± 4.0	6.07 ± 0.19	7.05	0−0
2929.55 ± 0.10	82.3 ± 5.2	3.90 ± 0.25	7.07	1−0
2939.70 ± 0.10	164.0 ± 7.5	7.80 ± 0.36	6.75	1−1
2947.85 ± 0.10	73.5 ± 3.0	3.48 ± 0.14	7.08	1−1
2956.7 ± 0.2	10.9 ± 0.4	0.52 ± 0.02	7.88	1−
2965.6 ± 0.2	48.4 ± 2.5	2.29 ± 0.12	7.22	1+1
2969.5 ± 0.2	13.2 ± 0.9	0.63 ± 0.04	7.77	(2−2)
2975.2 ± 0.2	16.9 ± 1.2	0.80 ± 0.06	7.65	(0, 1−)
3007.2 ± 0.2	7.6 ± 0.4	0.36 ± 0.02	7.96	
3042.6 ± 0.2	3.5 ± 0.3	0.17 ± 0.01	8.19	
3065.1 ± 0.2	4.6 ± 0.2	0.22 ± 0.01	8.02	
3067.2 ± 0.2	7.6 ± 0.5	0.36 ± 0.02	7.81	
3099.6 ± 0.1	35.8 ± 1.8	1.70 ± 0.09	7.05	
3115.2 ± 0.2	45.6 ± 2.3	2.16 ± 0.11	6.90	1−0
3131.0 ± 0.2	6.4 ± 0.7	0.31 ± 0.03	7.66	
3140.6 ± 0.3	8.0 ± 0.3	0.38 ± 0.01	7.54	
3146.2 ± 0.2	8.2 ± 0.6	0.39 ± 0.03	7.51	
3149.2 ± 0.2	13.1 ± 0.8	0.62 ± 0.04	7.30	(1−0)
3165.6 ± 0.10	25.3 ± 1.7	1.20 ± 0.08	6.96	1−1
3169.6 ± 0.3	0.8 ± 0.1	0.04 ± 0.005	8.43	
3179.8 ± 0.2	11.3 ± 1.0	0.54 ± 0.05	7.27	
3186.7 ± 0.2	12.8 ± 0.8	0.61 ± 0.04	7.20	
3195.5 ± 0.2	9.0 ± 0.9	0.43 ± 0.04	7.32	(1−0)
3274.4 ± 0.4	2.2 ± 0.2	0.10 ± 0.01	7.64	
3302.6 ± 0.4	0.8 ± 0.1	0.04 ± 0.005	7.74	
3314.1 ± 0.4	1.0 ± 0.1	0.05 ± 0.005	7.59	

TABLE IV. Comparison of level and $I\pi K$ assignments from this work and two other references.

This work	Mihelich (Ref. 13)	Bonch-Osmolovskaya (Ref. 12)	Our $I\pi K$	Mihelich $I\pi K$	Bonch-Osmolovskaya $I\pi K$
0	0	0	0 + 0	0 + 0	0 + 0
84.262	84.3	84.26	2 + 0	2 + 0	2 + 0
277.39	277.6	277.8	4 + 0	4 + 0	4 + 0
1069.40	1069.6	1069.1	0 + 0	0 + 0	0 + 0
1138.58	1138.5	1138.25	2 + 2	2 + 2	2 + 2
1145.65	1145.7	1145.5	2 + 0	2 + 0	2 + 0
1225.4	1225.2		3 + 2	3 + 2	
1228.9	1228.5	1228.4	0 + 0	0 + 0	0 + 0
1306.35	1306.3	1306.2	2 + 0	2 + 0	2 + 0
1364.55	1364.5	1364.2	1 − 0	1 − 0	1 − 0
1397.0					
1425.30	1425.5		2 − 2	2 − (2)	
1479.90	1480.0	1479.6	0 + 0	0 + 0	0 + 0
1512.4	1512.0	1511.6	1 − 0	1 − 0	1 − 0
1534.53	1534.6	1534.2	2 + 0	2 + 0	2 + 0
1566.4	1566.3	1565.9	0 + 0	0 + 0	0 + 0
1634.8	1635.1	1634.8	(2 + 0)	0 − 0	2 + 0
1658.0					
1717.95	1717.9		2 − 2	2 − (1)	
		1757.6			2 + (2)
		1961.4			1 − 0
1985.6	1985.4		2 − (2)	(1−)	
2040.0	2040.2	2039.6	1 + 1	1 + 1	1 + 1
2052.6			0 − 0		
		2113.2			(2+)
2116.0			1 − 0		
2126.10	2126.2	2125.6	1 − 0	1 − 0	1 − 0
2200.8					
2268.1					
2275.4	2275.5	2275.1	1 − 0	1 − 0	1 − 0
2289.3					
2351.8			0 − 0		
	2352.3			1−, 2−	
2364.05	2364.2	2363.4	1 − (1)	1 − (0)	1 − (1)
2367.70	2367.8	2367.2	(0 − 0)	1−, 2−	1−
2400.15	2400.2	2399.1	1 − 1	1 − 1	1 − 1
2429.1			2+		
2496.15	2496.3	2496.0	1 − 1	1−	1 − (0)
2498.3	2498.0		(0 − 0)	1−, 2−	
		2521.3			(2+)
2522.9			(1+)		
		2533.1			1 + 0
2536.8			1 − (0)		
	2584.5			1+, 0+	
		2641.4			1+
2661.0					
2667.38			1 − 0		
2748.15	2748.2	2747.8	1 − 1	1 − 1	1 − 1
2768.3	2768.7			1−, 2−	
2775.7	2775.8	2775.3	1−	2−	2−
2783.0	2783.1	2782.6	1 + 1	1 + 1	1 + 1
2819.80	2819.8	2819.3	0 − 0	1−, 2−	1−
		2883.6			1+
2929.55	2929.9	2929.6	1 − 0	1 − 0	1 − 0
2939.70	2940.0	2939.2	1 − 1	1−	1 − (0)

TABLE IV *(Continued)*

This work	Mihelich (Ref. 13)	Bonch-Osmolovskaya (Ref. 12)	Our $I\pi K$	Mihelich $I\pi K$	Bonch-Osmolovskaya $I\pi K$
2947.85	2948.1	2947.5	1 − 1	1−	1 − (1)
2956.7			1−		
2965.6	2966.2	2965.3	1 + 1	1+	1 + 1
2969.5			0, 1−		
2975.2					
3007.2					
3042.6					
3065.1					
3067.2		3067.6			1−, 2−
	3092.5	3091.9		(1−)	1 + 1
3099.6	3100.0	3099.4		1+	1−
3115.2	3115.6	3114.7	1 − 0	1 − 0	1 − 0
3131.0					
3140.6					
3146.2		3148.3			1+
3149.2	3149.4		1 − 0	1+	
3165.6			1 − 1		
3169.6					
3179.8					
		3184.1			1+
3186.7					
3195.5	3195.7	3196	1 − 0	1+	1 − 0
3274.4	3274.8	3274.9		1−	1−
	3287			(0−)	
3302.6		3301.7			1+
3314.1			(1 + 1)		
		3336.5			1−
		3432.6			1−

ratio, supports the 1-0 assignment for the 1512.4-keV state.

1566.4- and 1634.8-keV states. The 1566.4- and 1634.8-keV states form the beginning of the fourth low-lying $K=0+$ excited band. Again, the $E0$ branches to the ground and first two excited 0+ states make the assignment of $0+0_4$ to the 1566.4-keV level unambiguous. Although the 1357.4-keV transition to the 4+ ground-band member is conspicuously absent from the 1634.8-keV level, the $E2$ character of the 1634.8-keV $2\rightarrow 0$ transition and the apparent $E0$ enhancement of the 1550.6-keV conversion coefficient argue strongly for an assignment of $2+0_4$ for this state.

1658.0-keV level. The 1658.0-keV level is the second state for which no definite spin and parity assignment is possible. Once again, as for the 1397.0-keV state, weak γ-ray branches to the 2+ and 4+ ground-band members are seen, but the conversion lines were not observed and little feeding occurs from higher-lying levels. This level may decay to the ground state, but unfortunately, a ^{169}Lu line occurs at the same energy, and a ground-state transition thus remains questionable. The logft is quite large, so a relatively high spin seems justified on this basis.

1718.0-keV state. A trio of $E1$ transitions deexcites the 1718.0-keV state into the $K=2+$ γ vibrational band and the apparently strongly mixed $2+0_1$ state at 1145.7-keV. The γ-ray branching ratios do not provide convincing support for the $K=2$ assignment, and it is therefore based largely on the absence of any observable feeding into the ground band.

Levels above 1800 keV. Beginning at 1985.6 keV, a multitude of low-spin states is populated by the ^{170}Lu decay. Most of these states appear to have 0 or 1 unit of angular momentum and odd parity. Several exhibit the peculiar γ-ray branching characteristic of 0-0 states. Strangely enough (in view of the four lower-lying 0+ excitations already discussed), no conclusive evidence for further population of 0+ excited states is seen. Thus, with but four exceptions, all the remaining levels in ^{170}Yb for which sufficient data are available appear to be either 0- or 1-. Abbreviated arguments for the assignments proposed for the remaining ^{170}Yb states populated in ^{170}Lu decay follow. In general, the remaining assignments are based on γ-ray multipolarities from K conversion coefficient data, selective feeding to lower-lying states of known $I\pi K$, and γ-ray branching ratios. Most of these higher-lying states must await considerable further information before any attempts can be made to understand their structure in detail.

States of $I\pi K = 0-0$. We propose 0− assignments for states at 2052.6, 2351.8, 2498.3, and 2819.8 keV. In every case, decay from these states picks out lower-lying $I\pi K = 1-0$ and $1-1$ states, or, in a few instances, states with $I\pi K = 2-2$. Decay to the ground band and other $K = 0+$ band members is strictly forbidden except for $M2$ or higher-order transitions that are not observed. The 0−0 assignment is also supported in each case by conversion data that indicate $M1$ multipolarity for the deexciting γ rays.

States of $I\pi K = 1-0$. In addition to the two low-lying 1−0 states at 1364.6 and 1512.4 keV, other such states are assigned at 2126.1, 2275.4, 2667.4, 2929.6, 3115.2, 3149.2, 3195.5, and possibly 2116.0 and 2536.8 keV. In those cases where we make definite assignments, one or more transitions to the ground or excited 0+ bands have been identified as $E1$, and the characteristic factor-of-two enhancement of the $1- \to 2+$ transition relative to the $1- \to 0+$ branch is observed. In the case of some of the higher-lying levels, assuming states of $I\pi K = 1+0$ do not occur (not necessarily a valid assumption, as we note later), feeding to the 0+ and 2+ ground-band members with the correct reduced-intensity ratio is considered sufficient to support the 1−0 assignment, even though the $E1$ character may not be established.

States with $I\pi K = 1-1$. The 1−1 assignment is established for states at 2400.1, 2496.1, 2748.2, 2939.7, 2947.8, 3165.6, and possibly 2364.0 keV. The basis is rather similar to that just discussed for the 1−0 levels, except that the reduced branching ratio of 0+ band members is now reversed to 2 : 1 in favor of the 0+ spin state. Generally, a greater tendency to feed states with $I\pi K = 2\pm 2$ is noted for the states assigned 1−1.

States with $I\pi K = 1+1$. At least three states of this interesting class of excitation are thought to be identified in ^{170}Yb. The states at 2040.0, 2783.0, and 2965.6 keV seem well characterized; $M1$ transitions are observed to feed the 0+ and 2+ ground-rotational-band members, with some $E2$ mixture apparent in the $1+ \to 2+$ transitions.

It is noteworthy that we are unable to identify any states of the 1+0 configuration, such as those proposed by Gabrakov, Kuliev, and Pyatov.[25] In particular, we fail to establish the existence of a state at 2533.1 keV previously proposed[12] to be the $I\pi K = 1+0$ two-quasineutron state of configuration $[\frac{5}{2}(523)_n\downarrow] - [\frac{5}{2}(512)_n\uparrow]$.

States with $I\pi = 2-$. Only one state with proposed spin of two units is definitely identified above 1800 keV, and the K quantum number assigned for this state must be considered tentative. The state at 1985.6 keV is assigned on the basis of the single γ ray of apparent $E1$ multipolarity leading to the ground-rotational-band 2+ state.

III. DISCUSSION OF THE ^{170}Yb LEVEL SCHEME

In the simplest sense, an overview of the level structure of the ^{170}Yb nucleus provides a graphical illustration of the distinction to be made between those excited states clearly influenced by coherent many-particle interactions and those whose structure may be dominated by essentially two or four quasiparticle configurations. Such a generalization is encouraged by the presumably fortuitous appearance of a distinct gap at about 1800 keV in the observed low-spin ^{170}Yb states. It is interesting to note that a similar phenomenon seems to occur in ^{176}Hf, another even-even deformed nucleus for which numerous low-spin states have been identified from radioactive decay.[26] In both nuclei, this dearth of at least low-spin states occurs near 2Δ, the upper limit of the pairing energy gap expected to be ~1.6 MeV for ^{176}Hf and ~1.7 MeV for ^{170}Yb. In both nuclei there also seems to be some evidence for a similar decrease in level density near the energy 4Δ.

At the present time, it is perhaps only for the lowest-lying group of excited states, those within the energy gap 2Δ, that one may hope for a degree of success in characterizing the exact nature of the observed states. This is particularly so in view of the uncertainty associated with the spin and parity assignments for many of the higher-lying levels. In the light of present understanding, we proceed to discuss the several classes of "collective" states seen in the ^{170}Yb level scheme and then we provide a brief comparison with the few published quantitative calculations attempted for this nucleus.

A. $K = 0+$ Excitations in ^{170}Yb

The observation in ^{170}Yb of four 0+ excitations, all presumably within the pairing energy gap 2Δ, lends further interest to the lively discussion that already surrounds the occurrence of multiple low-lying 0+ states in deformed nuclei. It is well known that the simplest quadrupole vibrational mode allows for only one such low-energy 0+ excitation, but it is also well known by now that numerous deformed nuclei exhibit multiple low-lying 0+ excitations. Various explanations for this phenomenon have been made by invoking the quadru-

TABLE V. Derived values of the $E0$-$E2$ branching parameter $X=\rho^2 R_0^4 e^2 (I_n 200|I'_m 0)/B(E2)$ for decay of $K=0+$ states in ^{170}Yb.

Level (keV)	$I_n\pi \xrightarrow{e^-} I_m\pi$ / $I_n\pi \xrightarrow{\gamma} I'_m\pi$	E_{e^-} (keV) / E_γ (keV) Transition energies	I_{e^-}/I_γ	X [a]
1069.4	$0_1+ \to 0_0+$ / $0_1+ \to 2_0+$	1069.4 / 985.1	$34(3)/1.2\times10^5$	0.0049(5)
1145.6	$2_1+ \to 2_0+$ / $2_1+ \to 0_0+$	1061.4 / 1145.8	$\le 10/3.9\times10^4$	≤ 0.0021 [b]
	$2_1+ \to 2_0+$ / $2_1+ \to 2_0+$	1061.4 / 1061.4	$\le 10/4.7\times10^4$	≤ 0.0017 [b]
	$2_1+ \to 2_0+$ / $2_1+ \to 4_0+$	1061.4 / 868.1	$\le 10/1.7\times10^3$	≤ 0.032 [b]
1228.9	$0_2+ \to 0_0+$ / $0_2+ \to 2_0+$	1228.9 / 1144.6	$94(9)/3.7\times10^4$	0.080(9)
1306.4	$2_2+ \to 2_0+$ / $2_2+ \to 0_0+$	1222.2 / 1306.3	$86 \le I_{e^-} \le 114/1.1\times10^4$	$0.085 \le X \le 0.14$ [c]
	$2_2+ \to 2_0+$ / $2_2+ \to 2_0+$	1222.2 / 1222.2	$114(12)/1.4\times10^4$	0.100(12) [b]
	$2_2+ \to 2_0+$ / $2_2+ \to 4_0+$	1222.2 / 1028.8	$86 \le I_{e^-} \le 114/1.8\times10^4$	$0.041 \le X \le 0.068$ [c]
1479.9	$0_3+ \to 0_0+$ / $0_3+ \to 2_0+$	1479.9 / 1395.6	$650(70)/4.9\times10^4$	0.94(11)
1534.5	$2_3+ \to 2_0+$ / $2_3+ \to 0_0+$	1450.2 / 1534.6	$870 \le I_{e^-} \le 910/2.0\times10^4$	$0.86 \le X \le 1.2$ [c]
	$2_3+ \to 2_0+$ / $2_3+ \to 2_0+$	1450.2 / 1450.2	$910(100)/3.5\times10^4$	0.64(8) [b]
	$2_3+ \to 2_0+$ / $2_3+ \to 4_0+$	1450.2 / 1257.2	$870 \le I_{e^-} \le 910/3.0\times10^4$	$0.55 \le X \le 0.77$ [c]
	$2_3+ \to 2_1+$ / $2_3+ \to 2_1+$	388.8 / 388.8	$53(6)/2.0\times10^3$	0.0031(3) [b]
	$2_3+ \to 2_2+$ / $2_3+ \to 2_2+$	228.0 / 228.0	$290(80)/800$	0.0039(5) [b]
1566.4	$0_4+ \to 0_0+$ / $0_4+ \to 2_0+$	1566.4 / 1482.2	$83(13)/1.4\times10^4$	0.54(9)
1634.8	$2_4+ \to 2_0+$ / $2_4+ \to 0_0+$	1550.6 / 1634.8	$24 \le I_{e^-} \le 31/2100$	$0.30 \le X \le 0.50$ [c]
	$2_4+ \to 2_0+$ / $2_4+ \to 2_0+$	1550.6 / 1550.6	$31(4)/1.0\times10^4$	0.101(13) [b]

[a] The error limits placed on X are based only on the assigned γ-ray and electron relative intensities. It should be noted that most authors extract values for the electronic factor, Ω_K in the expression for the nuclear monopole transition strength parameter $\rho^2 = W/\Omega_K$ from the graph (or a poor reproduction thereof) of W/ρ^2 in Ref. 29 (where W is the $E0$ transition probability). The inaccuracy of such a procedure (and an unfortunate misprint for the $Z=85$ line that should not affect any published results for $Z=70$) probably requires that a reading error of at least 10% also be assigned to the values Ω_K used in the calculation of X. For example, we read $\Omega_K = 1.3\times10^{11}$ sec^{-1} for 1069 keV, while the authors of Ref. 12 read 1.1×10^{11}.

[b] Assumes the $2 \to 2'$ γ-ray transition is pure $E2$.

[c] Limits based on assumptions of pure $M1$ or pure $E2$ for $2 \to 2'$ transitions.

pole-quadrupole, pairing, and spin-quadrupole interactions, and combinations and variations of all three phenomena.[26,27] On the basis of the considerable volume of literature treating the subject from the standpoint of both experiment and theory, the picture now seems to be developing that the low-lying 0+ states in the deformed regions are not so much pure states of any single type, but rather consist of mixed-mode excitations where the quadrupole vibrational strength in particular may often be spread over several close-lying states.

One of the more useful properties of $K=0+$ excitations that may be extracted from decay data is the ratio of monopole to quadrupole decay into other 0+ bands. The usual expression is that proposed by Rasmussen[28]:

$$X\left[\frac{B(E0;\,0'+\to 0_g+)}{B(E2;\,0'+\to 2_g+)}\right]=\frac{\rho^2 e^2 R_0^{\,4}}{B(E2;\,0'+\to 2_g+)}\,. \qquad (1)$$

Similar expressions, including the applicable angular momentum coupling coefficients, may be written for transitions from higher spin members of the $K=0+$ bands to the ground band, and for interband transitions between excited 0+ band members. Table V displays the X parameters deduced for ^{170}Yb. Perhaps the most notable departure from the theoretical values allowable for a "good" β vibration, $0.15 \leqslant X \leqslant 0.80$,[28] is the very small $X=0.005$ observed for the lowest 0+ excitation. It is also for this state that the isospin-forbidden Fermi β decay is most highly hindered.

The quadrupole vibrational strength of 0+ excitations may be sensed by Coulomb excitation, and in the case of ^{170}Yb we are fortunate to have preliminary results from the (^{16}O, ^{16}O$'\gamma$) work of Riedinger *et al.*,[30] as shown in Table VI. On the basis of these data, one would conclude that there is little β-vibrational character in the first ^{170}Yb 0+ excitation at 1069 keV, and considerably more in the second, at 1229 keV. It is most remarkable that the $2+0_1$ state apparently has a large $E2$ transition moment to the ground state, while the $0+0_1\to 2+0_0$ moment to ground is at least an order-of-magnitude smaller. This is again consistent with the picture already suggested that the $2+2_\gamma$ and $2+0_1$ states are strongly mixed.

TABLE VI. $B(E2)$ data for $K=0+$ states in ^{170}Yb (from Ref. 30).

$E_i\to E_f$	$I_i\pi K_i\to I_f\pi K_f$	$B(E2)$ e^2 fm^4	$B(E2)$ spu
g.s.→ 1138.5	$0+0_0\to 2+2_\gamma$	~440	1.5
g.s.→ 1145.6	$0+0_0\to 2+0_1$	~440	1.5
1069.4→ 84.3	$0+0_1\to 2+0_0$	<30	<0.1
1228.9→ 84.3	$0+0_2\to 2+0_0$	420 ± 80	1.44

With the aid of the $B(E2)$ data of Riedinger *et al.*, it is also possible to calculate the values $\rho(E0)$, the nuclear $E0$ matrix elements, for the first two 0+ excited states in ^{170}Yb. With use of Eq. (1), we obtain the results shown in Table VII. It should be noted that in deriving the values for ρ in Table VII, we have made the assumption

$$B(E2;\,0_n+\to 2_0+)=B(E2;\,0_0+\to 2_n+)\,.$$

If in fact a simple first-order correction to the reduced $E2$ transition moment is allowed, then one has[27]

$$B(E2;\,0_n+\to 2_0+)=B(E2;\,0_0+\to 2_n)\left(\frac{1+6z_0}{1-6z_0}\right)^2, \qquad (2)$$

where $z_0=(M_2/M_1)$ according to the first-order expansion of Mikhailov[31]:

$$B(E2;\,I+0_n\to I'+0_0) = (I200|I'0)^2\{M_1+M_2[I'(I'+1)-I(I+1)]\}^2\,. \qquad (3)$$

The relation (2) should be valid if a consistent value of the parameter z_0 is found to adequately describe the branching from the members of a given "β-vibrational" band. Table VIII shows that in ^{170}Yb, except for the second excited 0+ band, the various derived z_0 parameters are *not* consistent for branching from the 2+0 excited states into the ground band. The $2\to 2$ transitions are assumed to be pure $E2$. It would be most surprising if this assumption were eventually shown to be valid for all 2+0 states in ^{170}Yb.

In the case of the second excited 0+ band, a single value of z_0 [i.e., consistent values of M_1 and

TABLE VII. $E0$ matrix elements in ^{170}Yb.

Level	Energy (keV)	X	$B(E2;\,0\to 2)$ [b] e^2 fm^4	$\lvert\rho\rvert$
$0+0_1$	1069.4	0.0049 ± 0.0005	<30	<0.009
$2+0_0$	1145.6	≤0.0021 [a]	440	≤0.01
$0+0_2$	1228.9	$0.080\ \pm 0.009$	420 ± 80	0.13 ± 0.03

[a] Assumes the $2+0_1\to 2+0_0$ transition is pure $E2$. If this transition has $M1$ admixture, then ρ is still smaller. Similar calculations could be listed for the other e^--γ branches from this level (Table V), but in view of the uncertainty in the $2+0_1\to 2+0_0$ monopole conversion intensity, these data provide no additional information.

[b] From Ref. 30.

M_2 in Eq. (3)] is found to fit the limited data nearly perfectly, so we may be justified in using Eq. (2) to modify the calculated value of ρ. This correction is only 27% for ρ^2, so that ρ_{corr} is 0.15. The fact that a single mixing parameter seems to describe the γ-ray branching from the $2{+}0_2$ state and that one deduces the relatively large value of $\rho \simeq 0.15$ for this band argues further for the characterization of the second excited $K=0+$ state as predominantly quadrupole-vibrational in nature. One notes in Pyatov's tabulation of experimental data[27] that the presumed "good" β-vibrational states in ^{150}Sm, ^{152}Sm, ^{154}Sm, ^{154}Gd, and ^{156}Gd all have values of $\rho(E0)$ in the range 0.2 to 0.5.

The early work of Reiner[32] considered the collective monopole transition moment arising from quadrupole surface oscillations of an incompressible uniformly charged spheroid and predicted values of $\rho(E0)$ in the range 0.2 to 0.6 for the β-vibrational states in deformed nuclei. The more general calculations of Bès[33] and, most recently, of Kuliev and Pyatov[34] have not changed the expectation that excited 0+ states that may be characterized as β vibrations should exhibit relatively large $E0$ moments as well as large $E2$ transition moments.

It is unusual that in ^{170}Yb one is also able to see $E0$ transitions between excited 0+ states. In Table IX the monopole transition matrix elements for transitions between the excited 0+ states and the ground-band 0+ state are compared. There appears to be little difference in the monopole matrix elements between the various 0+ states in the cases where the $E0$'s could be observed. The greatest

TABLE VIII. z_0 parameters for γ-ray branching from excited $K=0+$ bands in ^{170}Yb.

Transitions	Energies (keV)	$B'(E2)/B(E2)$	Alaga's rule	z_0
1145.8-keV $2+0_1$ state				
$\frac{2+0_1\to 0+0_0}{2+0_1\to 2+0_0}$	1145.8/1061.4	0.566	0.699	0.016
$\frac{2+0_1\to 4+0_0}{2+0_1\to 2+0_0}$	868.1/1061.4	0.099	1.80	−0.60
$\frac{2+0_1\to 0+0_0}{2+0_1\to 4+0_0}$	1145.8/868.1	5.71	0.388	−0.048
1306.3 $2+0_2$ state				
$\frac{2+0_2\to 0+0_0}{2+0_2\to 2+0_0}$	1306.3/1222.2	0.549	0.699	0.020
$\frac{2+0_2\to 4+0_0}{2+0_2\to 2+0_0}$	1028.8/1222.2	2.97	1.80	0.020
$\frac{2+0_1\to 0+0_0}{2+0_1\to 4+0_0}$	1306.3/1028.8	0.185	0.388	0.020
1534.5 $2+0_3$ state				
$\frac{2+0_3\to 2+0_0}{2+0_3\to 2+0_0}$	1534.5/1450.2	0.440	0.699	0.034
$\frac{2+0_3\to 4+0_0}{2+0_3\to 2+0_0}$	1257.3/1450.2	1.78	1.80	−0.0005
$\frac{2+0_3\to 0+0_0}{2+0_3\to 4+0_0}$	1534.5/1257.3	0.247	0.388	0.012
1634.8 $2+0_4$ state				
$\frac{2+0_4\to 0+0_0}{2+0_4\to 2+0_0}$	1634.8/1550.6	0.160	0.699	0.087
$\frac{2+0_4\to 4+0_0}{2+0_4\to 2+0_0}$	(1357.4)/1550.6	<0.384	1.80	<−0.038
$\frac{2+0_4\to 0+0_0}{2+0_4\to 4+0_0}$	1634.8/(1357.4)	>0.416	0.388	<−0.002

departure of the value ρ^2 is shown for the $0_3+\to 0_1+$ transition, where the $E0$ strength is about 20% that to ground.

Finally, it is worth noting that the 0+ bands higher in energy exhibit larger moments of inertia, perhaps indicating their greater two-particle character as compared with the lower 0+ bands; the 1479.9-keV 0+ band, for example, exhibits a moment of inertia some 50% greater than that of the ground band.

One of the most useful probes of the nature of excited 0+ states is provided by the transfer of a single nucleon or pair of nucleons to populate excited 0+ bands in the residual nucleus. The (p,t), $(^3He,d)$, (α,t), (p,d), and similar reactions can be particularly useful in this regard. Preliminary $^{172}Yb(p,t)^{170}Yb$ pickup reaction data from Oothoudt, Hintz, and Vedelsby[35] have shown only that the two-neutron-transfer reaction cross section for 0+ states drops off sharply as one moves toward lighter Yb isotopes, until in ^{170}Yb only tentative identification can be made of the 1069.3-keV 0+ state. This state appears to be populated with a cross section only 1% that of the ground 0+ state. These data seem to argue against the presence of much neutron pairing-vibrational character in the $0+0_1$ state of ^{170}Yb, at least.

Recent data from $^{169}Tm(\alpha,t)^{170}Yb$ reaction studies carried out at the Michigan State Cyclotron Laboratory[36] indicate strong $l=2$ proton transfer into the same 1228.9-keV $2+0_2$ excited state we have tentatively identified as the best candidate for a ^{170}Yb β-vibrational state. Since the (α,t) reaction in this case should predominantly involve transfer of a proton into the $\frac{1}{2}+[411]^{169}$Tm ground-state orbital, this result seems difficult to harmonize with the supposed collective nature of the state in question. Transfer-reaction studies aimed at further elucidating the 0+ states in ^{170}Yb are continuing.

As the experimental data on 0+ states in deformed nuclei have become more complete in recent years, some attempts have been made to develop a theoretical understanding for them. In most cases, however, little is known about absolute $E0$ transition probabilities or the details of the nuclear wave functions associated with excited 0+ states, and it seems rather futile to attempt to further characterize the different 0+ levels in ^{170}Yb on the basis of the still rather limited experimental data. Some workers have published theoretical calculations for the ^{170}Yb 0+ states, and in Fig. 15 the results of Kuliev and Pyatov[34] are displayed. Kuliev and Pyatov invoked the spin-quadrupole residual force and investigated the effect of coupling β vibrations with excitations of the spin-quadrupole type. They also included estimates of the X parameters, which are shown with the associated levels in Fig. 15, but it should be noted that these calculations are very sensitive to interference between the different 0+ excitation modes. The X parameters also depend on the effective charge used for calculating the $E0$ and $E2$ moments, so it is difficult to distinguish between the ^{170}Yb 0+ states on the basis of these parameters alone. Kuliev and Pyatov also show results for 0+ states induced by coupling proton and neutron pairing-vibrational modes with the quadrupole mode. The lowest roots of these calculations are shown as dashed lines in Fig. 15. It is noteworthy that addition to their calculations of both the pairing and spin-quadrupole interactions succeeds in lowering one 0+ state to an energy near that of the β-vibrational state as calculated by Bès,[33] but this refinement still fails to reproduce the observed four low-lying 0+ states. Kuliev and Pyatov do, however, predict $B(E2)=1.3$ single-particle units and $\rho(E0)=0.16$ for the lowest (1240 keV) 0+ excitation. This state may correspond to that seen

TABLE IX. Relative reduced $E0$ transition probabilities, $\rho^2(E0)/\rho_0^2(E0)$, from $K=0+$ states with multiple $E0$'s.

Level	Transitions	Transition energies	Relative e^- intensity	$R(E0)=\frac{\rho^2(E0)}{\rho_0^2(E0)}$
1479.9	$\frac{0_3+\to 0_1+}{0_3+\to 0_0+}$	$\frac{410.5}{1479.9}$	$\frac{35\le I_{e^-}\le 48}{652}$	$0.18\le R\le 0.24$ [a]
	$\frac{0_3+\to 0_2+}{0_3+\to 0_0+}$	$\frac{251.0}{1479.9}$	$\frac{247}{652}$	1.7
1566.4	$\frac{0_4+\to 0_1+}{0_4+\to 0_0+}$	$\frac{497.1}{1566.4}$	$\frac{31\le I_{e^-}\le 43}{83}$	$1.2\le R\le 1.6$ [a]
	$\frac{0_4+\to 0_2+}{0_4+\to 0_0+}$	$\frac{338.0}{1566.4}$	$\frac{15}{83}$	0.73

[a] A weak γ ray was observed at this same energy. The limits correspond to an assumed $E1$ or $M1$ multipolarity for the γ ray.

experimentally at 1229 keV.

Mikoshiba *et al.*[37] also carried out calculations for 0+ excitations in rare-earth nuclei. These authors considered the effects of coupling the quadrupole and pairing field fluctuations to generate mixed-mode 0+ excitations. They show no explicit results of 0+ level calculations for the ^{170}Yb case, but the general pattern of their results for other nuclei seems to predict a single lower-lying 0+ state that does not in every case carry the bulk of the quadrupole collectivity. A series of higher-lying 0+ states, near or above the upper limit of the pairing gap 2Δ, is normally expected then, according to their results. For ^{170}Yb, as for most other nuclei near the middle of the rare-earth region of deformation, Mikoshiba *et al.*[37] note that the quadrupole sum rule is far from exhausted on the "β-vibrational" state, which carries no more than 60% of the collective quadrupole strength.

Bernthal, Rasmussen, and Hollander[26] also reported attempts at calculating the 0+ excited levels for the single case of ^{176}Hf by means of an exact diagonalization of the pairing and quadrupole interaction matrix in a seniority-zero subspace of nine-proton and nine-neutron Nilsson orbitals nearest the Fermi surface. The results of these preliminary calculations for ^{176}Hf seemed to explain a very large value of the X parameter for one of two low-lying 0+ states in that nucleus, but the theory could not account for another 0+ state at still lower energy, relative to the first. Similar calculations have now been attempted for ^{170}Yb, but in this case the results are even more difficult to interpret in the absence of detailed $B(E2)$, $\rho(E0)$, and transfer-reaction data, or of unusual β- or γ-decay patterns that might label any of the ^{170}Yb 0+ states as being of one particular type or another.

In summary, it can be said that data of the kind required to resolve the problem of the multiple low-lying 0+ states in deformed nuclei are now becoming available, but much more work will be required before these states in ^{170}Yb and other deformed nuclei can be characterized in detail.

B. 2+2 γ-Vibrational Band

The experimental location of the γ-vibrational band head in ^{170}Yb is very close to that predicted by Bès *et al.*[38] It should be noted that some ambiguity still exists regarding the assignment of the 1138.6- or 1145.6-keV state as the γ-vibrational state, because of the failure of Alaga's branching rules to dictate one choice or the other. The breakdown of the geometrical branching relations for the transitions from these two states into the ground band may well indicate very strong mixing between the close-lying $2{+}0_1$ and $2{+}2_\gamma$ excited states. It is fashionable to gauge the degree of first-order mixing of the ground band into the γ-vibrational band by calculating the so-called z_2

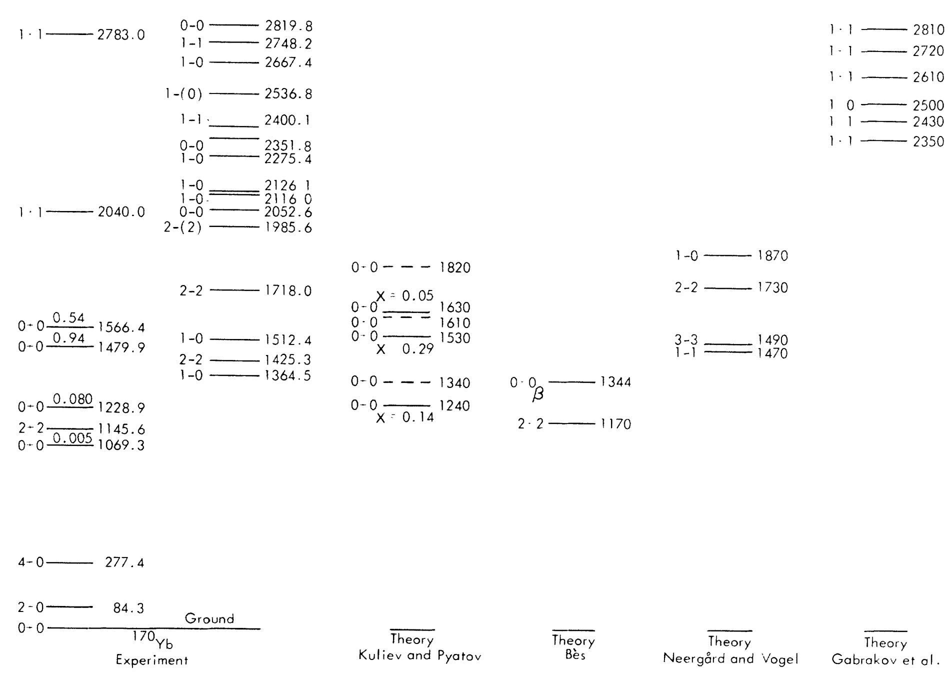

FIG. 15. Comparison of ^{170}Yb levels with theory from Kuliev and Pyatov (Ref. 34), Bès (Refs. 33 and 38), Neergård and Vogel (Ref. 40), and Grabakov, Kuliev, and Pyatov (Ref. 25).

parameter. The appropriate first-order expansion of the reduced $E2$ moment is similar to that written earlier for mixing between ground and excited 0+ bands[31]:

$$B(E2; I\pi 2_\gamma \to I'\pi 0) = 2(I22-2|I'0)^2|M_1 + M_2[I'(I'+1) - I(I+1)]|^2 , \quad (4)$$

where M_1 and M_2 are proportional to the principal and first-order $E2$ transition matrix elements. The z_2 parameter is then defined as

$$z_2 = [2M_2/(M_1 - 4M_2)] .$$

For ^{170}Yb, we find $z_2 = 0.052$ for transitions from the 2+2 state into the ground-rotational band, and $z_2 = 0.054$ for transitions from the 3+2 state. The expression of Mikhailov *et al.* and equivalent earlier relations involving the z parameter assume that the intrinsic quadrupole moments of the ground and γ-vibrational bands are equal. Reich and Cline[39] worked out the expressions whereby one may compare $z_2(0)$ with $z_2(2)$ for the presumed first-order mixing into the γ-vibrational band, where

$$z_2(0) \propto (Q_{00}/Q_{20})$$

and

$$z_2(2) \propto (Q_{22}/Q_{20}) ,$$

with Q_{00} and Q_{22} representing the intrinsic quadrupole moments of the ground and γ-vibrational bands, respectively, and Q_{20} the $E2$ transition moment between the two bands. Within the precision of the experimental data, no difference is found between $z_2(0)$ and $z_2(2)$ for the ^{170}Yb γ-vibrational band. Still, it is noteworthy that the simple first-order mixing theory predicts an intensity of 3500 units for the unseen 861.6-keV (2+2)→ (4+0) transition, a factor of 6 greater than the experimental upper limit for the intensity. The intensity of this unseen transition is in serious disagreement with Alaga's branching rules, and it is evident that the first-order mixing theory does not explain the discrepancy.

C. Low-Lying States of Odd Parity

Of the numerous odd-parity states excited in ^{170}Yb by ^{170}Lu decay, those states within or slightly above the energy gap 2Δ and thought to be influenced by the octupole-octupole interaction lend themselves most readily to interpretation. Neergård and Vogel[40] carried out extensive collective-model calculations for the octupole states in deformed even-even nuclei. They used a pairing and octupole-octupole residual force and solved the random-phase equations for quasiparticles in a Nilsson deformed potential well. With use of the intrinsic wave functions thus obtained, they also calculated the Coriolis interaction matrix elements and diagonalized the interaction matrix for the lowest-lying multiplet of octupole states: $K\pi = 0-$, 1−, 2−, and 3−. Their calculated energies for the members of this quartet of states in ^{170}Yb are shown in Fig. 15.

Perhaps the most puzzling feature of the ^{170}Yb level scheme in comparison with the calculations of Neergård and Vogel is the apparent presence of two states of $I\pi K = 1-0$, quite low in energy, at 1364 and 1512 keV. Such states are not particularly collective in this region, however, and Neergård and Vogel emphasize the extreme sensitivity of their calculations to the two-quasiparticle energies for single-particle states near the Fermi surface. This explanation may account for the 500-keV discrepancy between the calculated and the experimental location of the lowest 1−0 state in ^{170}Yb. The remaining anomaly, the apparent presence of a second 1−0 state at low energy, might be explained as resulting from strong mixing between the several low-lying odd-parity states in this region. The experimental assignment of zero K quantum numbers to the two states in question depends largely on γ-ray branching ratio data. In the case of the 1364-keV state, the data seem unassailable – the expected 2 : 1 favored feeding to the 2+0 ground-rotational-band member is very clear. In the case of the 1512-keV state, however, there is some room for doubt, though the 1− → 2+ reduced transition strength is still 60% greater than the 1− → 0+ strength, and far from the 50% smaller value that would imply a $K = 1$ assignment. The inclination to identify this state with the 1−1 octupole branch is further strengthened by our failure to identify any other 1−1 state below 2400 keV.

The lowest 2−2 root in ^{170}Yb is predicted in Ref. 39 to lie at 1730 keV; we observe 2−2 states at both 1425 and 1718 keV. Finally, it seems unlikely that we could identify the 3−3 octupole branch as being either of the two spin-three states tentatively proposed at 1397 and 1658 keV, since both states decay primarily into the $K = 0$ ground-rotational band.

D. States of $I\pi = 1+$

We have already noted the recent work of Gabrakov, Kuliev, and Pyatov[25] wherein the properties of excited states of the type of $I\pi = 1+$ with $K = 0$ or 1 are calculated. These authors show predicted energies of numerous states with $I\pi K = 1+1$ in ^{170}Yb, and although all of these states are predicted to be predominantly two-quasiparticle structures, in many cases they may also possess a weak collectivity proposed to arise from oscillations of the spin part of the nuclear magnetic dipole moment. The bulk of the strength of these collective oscillations is predicted to lie near 10 MeV, but smaller influences are expected at lower energies and would be evidenced primarily by enhanced $M1$ moments and hindered β feeding.[25]

Shown in Fig. 15 are only the lowest few 1+ states predicted by Gabrakov, Kuliev, and Pyatov to exist in ^{170}Yb. Others are proposed to lie at 2930, 2990, 3030, 3200, 3330, 3350, 3500, and 3520 keV. Only two of these states are predicted to have $K=0$ quantum numbers: one at 2500 keV and the other at 3520 keV.

In comparing the calculations of Gabrakov, Kuliev, and Pyatov with our experimental results, we can draw at least two conclusions: (1) Very few states of even parity appear to be directly populated by ^{170}Lu β decay. In fact, only four such states are identified in our work. This would appear to bear out the expectation that β decay to such states will be highly hindered.[25] (2) Bonch-Osmolovskaya *et al.*[12] propose a state at 2533.1 keV and assign to it the 1+0 $[\frac{5}{2}(523)_n\downarrow - \frac{5}{2}(512)_n\uparrow]$ two-neutron configuration proposed by Ref. 25. We fail to observe any state at 2533.1 keV, thus negating the earlier-suggested experimental identification of a state $I\pi K = 1{+}0$ in this nucleus. Such a state would be expected to be part of a rotational sequence 1, 3, 5, . . . , with even parity.[25]

IV. CONCLUSIONS

The staggering complexity of the ^{170}Yb level scheme raises the question of the feasibility and even the necessity of experimentally detailing the structure of the myriad excited states in this and other similarly complex nuclei. The objective of an increased understanding of structure in such nuclei is perhaps best achieved by concentrating further study on a few of the states most representative and perhaps least understood of a particular type of excitation or interaction. In ^{170}Yb, the best candidates for such detailed further investigations are those states lying within the energy gap 2Δ. High-resolution direct-reaction particle spectroscopy can reveal much about the exact nature of the four low-lying 0+ states. Coulomb-excitation studies with ions heavier than ^{16}O may shed still more light on the structure of these interesting states. It is also of interest to further detail the nature of the low-lying odd-parity states, in order to better define the structure of the various octupole collective-vibrational modes. Higher-lying states meriting additional study include the 1+1 and 1+0 excitations. It would be of considerable interest to be able to document the proposed collective properties of these states. Finally, one must note again the curious gaps in the level structures of both ^{170}Yb and ^{176}Hf that seem to occur near the energies 2Δ and perhaps also 4Δ. It is important to determine from further study in ^{170}Yb and other nuclei whether this feature is indeed fortuitous, a result only of selective β-decay feeding perhaps, or whether it represents a more general phenomenon that may provide new insight into the pairing interaction in nuclei.

ACKNOWLEDGMENTS

The authors wish to thank Jesse Meadows for the excellent chemical separations and Paul Johnson for his many efforts that led to a successful isotopic separation. We also wish to express our appreciation to Keith Grant for his analysis of the conversion-electron data, Dr. Jorma Routti for his assistance in operating VISTA, Lou Maynard for his assistance with the experimental equipment, and Allan Van Lehn for assistance with SAMPO on the Livermore computers. Discussions with Professor J. O. Rasmussen were both stimulating and helpful. We thank Dr. Lee Riedinger for permission to cite preliminary results from his ^{170}Yb Coulomb-excitation studies. Special thanks are due Dr. Lloyd Mann for aid in the final stages of preparing the manuscript. One of us (FMB) thanks the members of the Radiochemistry Division of the Lawrence Livermore Laboratory for their hospitality during a brief but fruitful visit in August of 1970.

Part of the work reported here was carried out at the Lawrence Berkeley Laboratory.

†Work performed under the auspices of the U. S. Atomic Energy Commission at the Lawrence Laboratories and at Michigan State University under Contract No. AT(11-1)-1779.

*On leave of absence, September 1971–August 1972, to Interuniversitair Reactor Instituut, Delft, Netherlands.

[1]B. S. Dzhelepov, A. I. Medvedev, S. A. Shestopalova, and I. F. Uchevatkin, Nucl. Phys. 56, 283 (1964).

[2]B. Harmatz, T. H. Handley, and J. W. Mihelich, Phys. Rev. 119, 1345 (1960).

[3]V. V. Tuchkevich, V. A. Romanov, and M. G. Iodko, Izv. Akad. Nauk SSSR, Ser. Fiz. 24, 1457 (1960) [transl.: Bull. Acad. Sci. USSR, Phys. Ser. 24, 1451 (1960)].

[4]N. A. Bonch-Osmolovskaya, J. Vrzal, E. P. Grigoriev, N. G. Zayseva, J. Liptak, B. G. Tishin, and J. Urbanec, Joint Institute for Nuclear Research Report No. 6-3452,

1967 (unpublished).

[5]B. S. Dzhelepov, V. E. Ter-Nersesyants, and S. A. Shestopalova, Izv. Akad. Nauk SSSR, Ser. Fiz. 31, 1633 (1967) [transl.: Bull. Acad. Sci. USSR, Phys. Ser. 31, 1673 (1967)].

[6]V. A. Balalaev, B. S. Dzhelepov, A. I. Medvedev, V. E. Ter-Nersesyants, I. F. Uchevatk, and S. A. Shestopalova, Izv. Akad. Nauk SSSR Ser. Fiz. 32, 730 (1968) [transl.: Bull. Acad. Sci. USSR, Phys. Ser. 32, 671 (1969)].

[7]B. S. Dzhelepov, V. E. Ter-Nersesyants, and S. A. Shestopalova, Izv. Akad. Nauk SSSR, Ser. Fiz. 33, 2 (1969) [transl.: Bull. Acad. Sci. USSR, Phys. Ser. 33, 3 (1969)].

[8]D. C. Camp and F. M. Bernthal, Bull. Am. Phys. Soc. 15, 522 (1970).

[9]P. G. Hansen, H. L. Nielsen, K. Wilsky, and J. Treherne, Phys. Letters 19, 304 (1965).

[10]C. J. Paperiello, E. G. Funk, J. W. Mihelich, and G. Schiling, in *Proceedings of the International Conference on Properties of Nuclear States, Montréal, Canada, 1969* (Presses de l'Université de Montréal, Montréal, Canada, 1969).

[11]N. Bonch-Osmolovskaya, H. Ballund, A. Zglinski, A. Plochocki, and Z. Preibisz, Joint Institute for Nuclear Research Report No. P6-4773, 1969 (unpublished).

[12]N. A. Bonch-Osmolovskaya, H. Ballund, A. Plochocki, Z. Preibisz, and A. Zglinski, Nucl. Phys. A162, 305 (1971).

[13]J. W. Mihelich, private communication.

[14]Reference to a company or product name does not imply approval or recommendation of the product by the University of California or the U. S. Atomic Energy Commission to the exclusion of others that may be suitable.

[15]D. C. Camp, in *Proceedings of the International Conference on Radioactivity in Nuclear Spectroscopy* (Gordon and Breach, N.Y., 1971); also, Lawrence Livermore Laboratory Report No. UCRL-71825, 1969 (unpublished).

[16]L. B. Robinson, F. Gin, and H. Cingolani, Nucl. Instr. Methods 75, 121 (1969); L. B. Robinson, F. Gin, and F. S. Goulding, Nucl. Instr. 62, 237 (1968); F. M. Bernthal, Lawrence Berkeley Laboratory Report No. UCRL-18651, 1969 (unpublished).

[17]J. T. Routti, Lawrence Berkeley Laboratory Report No. UCRL-19452, 1969 (unpublished).

[18]J. T. Routti and S. G. Prussin, Nucl. Instr. Methods 72, 125 (1969).

[19]The VISTA hardware consists of a large TV screen, a function-control box and a light pen. The light pen allows the user to interact with the data shown on the TV screen and to exercise through the function-control box any program option of SAMPO.

[20]R. Gunnink, R. A. Meyer, J. B. Niday, and R. P. Anderson, Nucl. Instr. Methods 65, 26 (1968).

[21]D. C. Camp and F. M. Bernthal, Lawrence Livermore Laboratory Report No. UCRL-72295 (1971).

[22]M. A. S. Mariscotti, G. Scharff-Goldhaber, and B. Buck, Phys. Rev. 178, 1864 (1969).

[23]D. G. Burke and B. Elbek, Kgl. Danske Videnskab. Selskab, 36, No. 6 (1967).

[24]C. M. Lederer, J. M. Hollander, and I. Perlman, *Table of Isotopes* (Wiley, New York, 1967), 6th ed.

[25]S. I. Gabrakov, A. A. Kuliev, and N. I. Pyatov, Yadern. Fiz. 12, 82 (1971) [transl.: Soviet J. Nucl. Phys. 12, 44 (1971)]; to be published; Joint Institute for Nuclear Research Report No. E4-4908, 1970 (unpublished).

[26]F. M. Bernthal, J. O. Rasmussen, and J. M. Hollander, Bull. Am. Phys. Soc. 15, 523 (1970).

[27]For a summary of current thinking on these different approaches see N. I. Pyatov, Joint Institute for Nuclear Research Report No. P4-5422, 1970 (unpublished); B. S. Dzhelepov and S. A. Shestopalova, in *Proceedings of the International Symposium on Nuclear Structure, Dubna, 1968* (International Atomic Energy Agency, Vienna, 1969), p. 39; S. T. Belyaev, *ibid.*, p. 155.

[28]J. O. Rasmussen, Nucl. Phys. 19, 85 (1960).

[29]E. L. Church and J. Weneser, Phys. Rev. 103, 1035 (1956).

[30]L. Riedinger, G. Schilling, A. E. Rainis, E. G. Frank, and J. W. Mihelich, private communication of preliminary results.

[31]V. M. Mikhailov, Izv. Akad. Nauk SSSR Ser. Fiz. 30, 1334 (1966) [transl.: Bull. Acad. Sci. USSR, Phys. Ser. 30, 1392 (1966).

[32]A. S. Reiner, Nucl. Phys. 27, 115 (1961).

[33]D. R. Bès, Nucl. Phys. 49, 544 (1963).

[34]A. A. Kuliev and N. I. Pyatov, Izv. Akad. Nauk SSSR Ser. Fiz. 32, 831 (1969) [transl.: Bull. Acad. Sci. USSR, Phys. Ser. 32, 767 (1969)].

[35]M. Oothoudt, N. M. Hintz, and P. Vedelsby, Phys. Letters 32B, 270 (1970).

[36]F. M. Bernthal, work in progress.

[37]O. Mikoshiba, R. K. Sheline, T. Udagawa, and S. Yoshida, Nucl. Phys. A101, 202 (1967).

[38]D. R. Bès, P. Federman, E. Maqueda, and A. Zuker, Nucl. Phys. 65, 1 (1965).

[39]C. W. Reich and J. E. Cline, Idaho Nuclear Corporation Report No. IN-1317 (1970).

[40]K. Neergård and P. Vogel, Nucl. Phys. A145, 33 (1970).